



General one-loop formulas for $H \rightarrow f \bar{f} \gamma$ and its applications

Vo Van On^{1,a}, Dzung Tri Tran², Chi Linh Nguyen², Khiem Hong Phan^{3,4,b}

¹ Institute of Applied Technology, Thu Dau Mot University, Thu Dau Mot City, Binh Duong 75000, Vietnam

² University of Science Ho Chi Minh City, 227 Nguyen Van Cu, District 5, Ho Chi Minh City, Vietnam

³ Institute of Fundamental and Applied Sciences, Duy Tan University, Ho Chi Minh City 700000, Vietnam

⁴ Faculty of Natural Sciences, Duy Tan University, Da Nang City 550000, Vietnam

Received: 15 November 2021 / Accepted: 18 March 2022 / Published online: 31 March 2022

© The Author(s) 2022

Abstract General one-loop contributions to the decay processes $H \rightarrow f \bar{f} \gamma$ and its applications are presented in this paper. We consider all possible contributions of the additional heavy vector gauge bosons, heavy fermions, and charged (also neutral) scalar particles propagating in Feynman loop diagrams. Therefore, analytic results are valid in a wide class of models beyond the Standard Model. Analytic formulas for the form factors are expressed in terms of Passarino-Veltman functions in the standard notations of LoopTools. Hence, the decay rates can be evaluated numerically by using this package. The computations are then applied to the cases of the Standard Model, $U(1)_{B-L}$ extension of the Standard Model as well as Two Higgs Doublet Model. Phenomenological results for all the above models are studied. We observe that the effects of new physics are sizable contributions and these can be probed at future colliders.

1 Introduction

After discovering the Standard-Model-like (SM-like) Higgs boson [1, 2], one of the main purposes at future colliders like the high luminosity large hadron collider (HL-LHC) [3, 4] as well as future lepton colliders [5] is to probe the properties of this boson (mass, couplings, spin and parity, etc). In this experimental program, the Higgs productions and its decay rates should be measured as precisely as possible. Based on these measurements, we can verify the nature of the Higgs sector. In other words we can understand deeply the dynamic of the electroweak symmetry breaking. It is well-known that the Higgs sector is selected as the simplest case in the Standard Model (SM), since there is only one scalar doublet field. From theoretical viewpoints, there are no reasons for this simplest choice. Many models beyond the SM (BSMs) have

extended the Higgs sector (some of them have also expanded gauge sectors, introduced mass terms of neutrinos, etc). In these models many new particles are proposed, for examples, new heavy gauge bosons, charged and neutral scalar Higgs as well as new heavy fermions. These new particles may also contribute to the productions and decay of Higgs boson. Therefore, the more precise data on the Higgs productions and decay rates could provide us an important information to answer the nature of the Higgs sector and, more importantly, to extract the new physics contributions.

Among all the Higgs decay channels, the processes $H \rightarrow f \bar{f} \gamma$ are of great interest for the following reasons. Firstly, the decay channels can be measured at the large hadron collider [6–9]. Therefore, these processes can be used to test the SM at the high energy regions. Secondly, many of new particles as mentioned in the beginning of this section may also propagate in the loop diagrams of the decay processes. Subsequently, the decay rates could provide a useful tool for constraining new physics parameters. Last but not least, apart from the SM-like Higgs boson, new neutral Higgs bosons in BSMs may be mixed with the SM-like one. These effects can also be observed directly by measuring of the decay rates of $H \rightarrow f \bar{f} \gamma$. For above reasons, the detailed theoretical evaluations of one-loop contributions to the decay of Higgs to fermion pairs and a photon within the SM and its extensions are necessary.

Theoretical implications for the decay $H \rightarrow f \bar{f} \gamma$ in the SM at the LHC have been studied in Refs. [10–12]. Moreover, many computations of one-loop contributions to the decay processes $H \rightarrow f \bar{f} \gamma$ are available within the SM framework [13–20]. The same evaluations for the Higgs productions at $e\gamma$ colliders have been proposed in [21, 22]. One-loop corrections to $H \rightarrow f \bar{f} \gamma$ in the context of the minimal super-symmetric standard model Higgs sector have been computed in [23]. Furthermore, one-loop contributions for CP-odd Higgs boson productions in $e\gamma$ collisions have

^a e-mail: onvv@tdmu.edu.vn

^b e-mail: phanhongkhiem@duytan.edu.vn (corresponding author)

been carried out in [24]. In this article, we present general formulas for one-loop contributions to the decay processes $H \rightarrow f \bar{f} \gamma$. The analytic results presented in the current paper are not only valid in the SM but also in many BSMs in which new particles are proposed such as heavy vector bosons, heavy fermions, and charged (neutral) scalar particles that may propagate in the loop diagrams of the decay processes. The analytic formulas for the form factors are expressed in terms of Passarino-Veltman (PV) functions in standard notations of `LoopTools` [25]. As a result, they can be evaluated numerically by using this package. The calculations are then applied to the SM, the $U(1)_{B-L}$ extension of the SM [26] and two Higgs doublet models (THDM) [27]. Phenomenological results of the decay processes for these models are also studied.

We also stress that our analytical results in the present paper can also be applied to many more BSM frameworks. In particular, in the super-symmetry models, many superpartners of fermions and gauge bosons are introduced. Furthermore, with extending the Higgs sector, we encounter charged and neutral Higgs bosons in this framework. There exist extra charged gauge bosons in many electroweak gauge extensions, for examples, the left-right models (LR) constructed from the $SU(2)_L \times SU(2)_R \times U(1)_Y$ [28–30], the 3-3-1 models ($SU(3)_L \times U(1)_X$) [31–37], the 3-4-1 models ($SU(4)_L \times U(1)_X$) [37–42], etc. Analytic results in this paper have already included the contributions by such particles which may also be exchanged in the loop diagrams of the aforementioned decay processes. Phenomenological results for the decay processes in the above models are of great interest in future. Future publications will be devoted to these topics.

The layout of the paper is as follows: we first write down the general Lagrangian and introduce the notation for the calculations in the Sect. 2. We then present the detailed calculations for one-loop contributions to $H \rightarrow f \bar{f} \gamma$ in Sect. 3. The applications of this work to the SM, $U(1)_{B-L}$ extensions of the SM and THDM are also studied in this section. Phenomenological results for these models are analysed at the end of Sect. 3. Conclusions and outlook are presented in the Sect. 4. In appendices, we first review briefly $U(1)_{B-L}$ extensions of the SM and THDM. Feynman rules and all involved couplings in the decay processes are then shown.

2 Lagrangian and notations

In order to write down the general form of Lagrangian for a wide class of the BSMs, we start from the well-known contributions that appear in the SM. We then add the extra terms which are extended from the SM. For example, the two Higgs doublet model [27] adds a new Higgs doublet that predicts new charged and neutral scalar Higgs bosons; a model with

a gauge symmetry $U(1)_{B-L}$ which proposes a neutral gauge boson Z' , a neutral Higgs [26,43]; minimal left-right models with a new non-Abelian gauge symmetry for electroweak interactions $SU(2)_L \times SU(2)_R \times U(1)_{B-L}$ [28–30] introducing many new particles including charged gauge bosons, neutral gauge bosons and charged Higgs bosons. The mentioned particles give one-loop contributions to the decays under consideration.

In this section, Feynman rules for the decay channels $H \rightarrow f \bar{f} \gamma$ are derived for the most general extension of the SM with considering all possible contributions from the mentioned particles. In this computation, we denote V_i, V_j for extra charged gauge bosons, V_k^0 for neutral gauge bosons. Moreover, S_i, S_j (S_k^0) are charged (neutral) Higgs bosons respectively and f_i, f_j indicate fermions. In general, the classical Lagrangian contains the following parts:

$$\mathcal{L} = \mathcal{L}_f + \mathcal{L}_G + \mathcal{L}_\Phi + \mathcal{L}_Y \tag{1}$$

where the fermion sector is given by

$$\mathcal{L}_f = \bar{\psi}_f i \not{D} \psi_f \tag{2}$$

with $D_\mu = \partial_\mu - \sum_V i g_V \left[\sum_a T^a V_\mu^a \right]$. In this formula, T^a is a generator of the corresponding gauge symmetry. The gauge sector reads

$$\mathcal{L}_G = -\frac{1}{4} \sum_V \left[\sum_a V_{\mu\nu}^a V^{a,\mu\nu} \right], \tag{3}$$

where $V_{\mu\nu}^a = \partial_\mu V_\nu^a - \partial_\nu V_\mu^a + g f^{abc} V_\mu^b V_\nu^c$ with f^{abc} being a structure constant of the corresponding gauge group. The scalar sector is expressed as follows:

$$\mathcal{L}_\Phi = \sum_\Phi Tr[(D_\mu \Phi)^\dagger (D^\mu \Phi)] - V(\Phi). \tag{4}$$

We then derive all the couplings from the full Lagrangian. The couplings are parameterized in general forms and presented as follows:

- By expanding the fermion sector, we can derive the vertices of vector boson V with fermions. In detail, the interaction terms are parameterized as

$$\mathcal{L}_{Vff} = \sum_{f_i, f_j, V} \bar{f}_i \gamma^\mu (g_{Vff}^L P_L + g_{Vff}^R P_R) f_j V_\mu + h.c. \tag{5}$$

with $P_{L,R} = (1 \mp \gamma_5)/2$ and $h.c$ is hermitian conjugate terms.

- Trilinear gauge and quartic gauge couplings are expanded from the gauge sector:

$$\begin{aligned}
 & \mathcal{L}_{VVVV, VVVV} \\
 &= \sum_{V_k^0, V_i, V_j} g_{V_k^0 V_i V_j} \left[(\partial_\mu V_{k,v}^0) V_i^\mu V_j^\nu \right. \\
 & \quad \left. + V_{k,v}^0 V_i^\mu (\partial^\nu V_{j,\mu}) + \dots \right] \\
 & \quad + \sum_{V_k^0, V_l^0, V_i, V_j} g_{V_k^0 V_l^0 V_i V_j} \left[V_{k,\mu}^0 V_{l,\nu}^0 V_i^\mu V_j^\nu + \dots \right] + \\
 & \quad + \sum_{V_k, V_l, V_i, V_j} \left[g_{V_k V_l V_i V_j} V_{k,\mu} V_{l,\nu} V_i^\mu V_j^\nu + \dots \right] \\
 & \quad + \dots
 \end{aligned} \tag{6}$$

- Next, the couplings of scalar S (S can be neutral or charged scalar) to fermions are taken from the Yukawa part \mathcal{L}_Y . The interaction terms are expressed as follows:

$$\mathcal{L}_{Sf_i f_j} = \sum_{f_i, f_j, S} \bar{f}_i (g_{Sf_i f_j}^L P_L + g_{Sf_i f_j}^R P_R) f_j S + h.c. \tag{7}$$

- The couplings of scalar S to vector boson V can be derived from the kinematic term of the Higgs sector. In detail, we have the interaction terms

$$\begin{aligned}
 \mathcal{L}_{SVV, SSV, SSVV} &= \sum_{S_k^0, V_i, V_j} g_{S_k^0 V_i V_j} S_k^0 V_i^\mu V_{j,\mu} \\
 & \quad + \sum_{S_i^0, S_j, V} g_{S_i^0 S_j V_k} [(\partial_\mu S_i^0) S_j - (\partial_\mu S_j) S_i^0] V_k^\mu \\
 & \quad + \sum_{S_k, V_i, V_j^0} g_{S_k V_i V_j^0} S_k V_i^\mu V_{j,\mu}^0 \\
 & \quad + \sum_{S_i, S_j, V^0} g_{S_i S_j V_k^0} [(\partial_\mu S_i) S_j - (\partial_\mu S_j) S_i] V_k^{0,\mu} \\
 & \quad + \sum_{S_i, S_j, V_k, V_l} g_{S_i S_j V_k V_l} S_i S_j V_k^\mu V_{l,\mu} \\
 & \quad + \sum_{S_i, S_j, V_k^0, V_l^0} g_{S_i S_j V_k^0 V_l^0} S_i S_j V_k^{0,\mu} V_{l,\mu}^0 \\
 & \quad + \sum_{S_i^0, S_j^0, V_k, V_l} g_{S_i^0 S_j^0 V_k V_l} S_i^0 S_j^0 V_k^\mu V_{l,\mu} \\
 & \quad + \sum_{S_i^0, S_j^0, V_k^0, V_l^0} g_{S_i^0 S_j^0 V_k^0 V_l^0} S_i^0 S_j^0 V_k^{0,\mu} V_{l,\mu}^0 \\
 & \quad + \dots
 \end{aligned} \tag{8}$$

- Finally, the trilinear scalar and quartic scalar interactions are from the Higgs potential $V(\Phi)$. The interaction terms are written as

$$\begin{aligned}
 \mathcal{L}_{SSS, SSSS} &= \sum_{S_k^0, S_i, S_j} g_{S_i S_j S_k} S_k^0 S_i S_j \\
 & \quad + \sum_{S_i^0, S_j^0, S_k, S_l} g_{S_i^0 S_j^0 S_k S_l} S_i^0 S_j^0 S_k S_l
 \end{aligned}$$

$$\begin{aligned}
 & + \sum_{S_i^0, S_j^0, S_k^0} g_{S_i^0 S_j^0 S_k^0} S_i^0 S_j^0 S_k^0 \\
 & + \sum_{S_i^0, S_j^0, S_k^0, S_l^0} g_{S_i^0 S_j^0 S_k^0 S_l^0} S_i^0 S_j^0 S_k^0 S_l^0 \\
 & + \sum_{S_i, S_j, S_k, S_l} g_{S_i S_j S_k S_l} S_i S_j S_k S_l + \dots \tag{9}
 \end{aligned}$$

All of the Feynman rules corresponding to the above couplings giving one-loop contributions to the SM-like Higgs decays $H \rightarrow f \bar{f} \gamma$ are collected in Appendix D. In detail, the propagators that appear in the decay processes in the unitary gauge are shown in Table 6. All the related couplings that occur in the decay are parameterized in general forms which are presented in Table 7 (we refer to appendices B and C for two typical models).

3 Calculations

In this section, one-loop contributions to the decay processes $H \rightarrow f(q_1) \bar{f}(q_2) \gamma(q_3)$ are calculated in detail. In the present paper, we consider the computations in the limit of $m_f \rightarrow 0$ for external fermions. All Feynman diagrams involving these processes can be grouped into the following classes (see Fig. 1).

By working in on-shell renormalization scheme, we confirm that the contribution of diagrams ($e + h$) vanishes for on-shell external photon, as explained in Refs. [44, 45]. One can neglect the Yukawa couplings y_f (since $m_f \rightarrow 0$ for external fermions) in this computation. As a result, the contributions of diagrams ($g + k$) can be omitted. Following Refs. [44, 45], it is known that we need a counterterm to get a finite result for these processes, because there exist tree level coupling HZZ and renormalization of mixing $Z\gamma$. The counterterm is depicted in the diagram (m) and its amplitude takes the form of $\sim g_{\mu\nu} C_{HZZ\gamma}$. As discussed in many previous works [13, 15, 17, 23, 46], if we collect the form factors as the coefficients of $q_3^\mu q_k^\nu$ in Eq. (10), the form factors do not receive any contribution from the counterterm diagram (m). Moreover, total contribution from the class ($a + f$) is vanishing. We also consider the group of ($n + o$) that is not equal to zero (as the group of ($a + f$)). However, we know that the couplings of $S_k^0 f \bar{f}$ are proportional to m_f/v (v is Vacuum Expectation Value). As a result, this contribution is also omitted in the limit of $m_f \rightarrow 0$. Hence, we only have the contributions of ($b + c + d$) which are separated into two kinds. The first one is the topology b which is called V_k^{0*} pole contributions. The second type (diagrams c and d) belongs to the non- V_k^{0*} pole contributions. We remind that V_k^{0*} can include both Z, γ in the SM and the arbitrary neutral vector boson Z' in many BSMs. In the further course, we consider

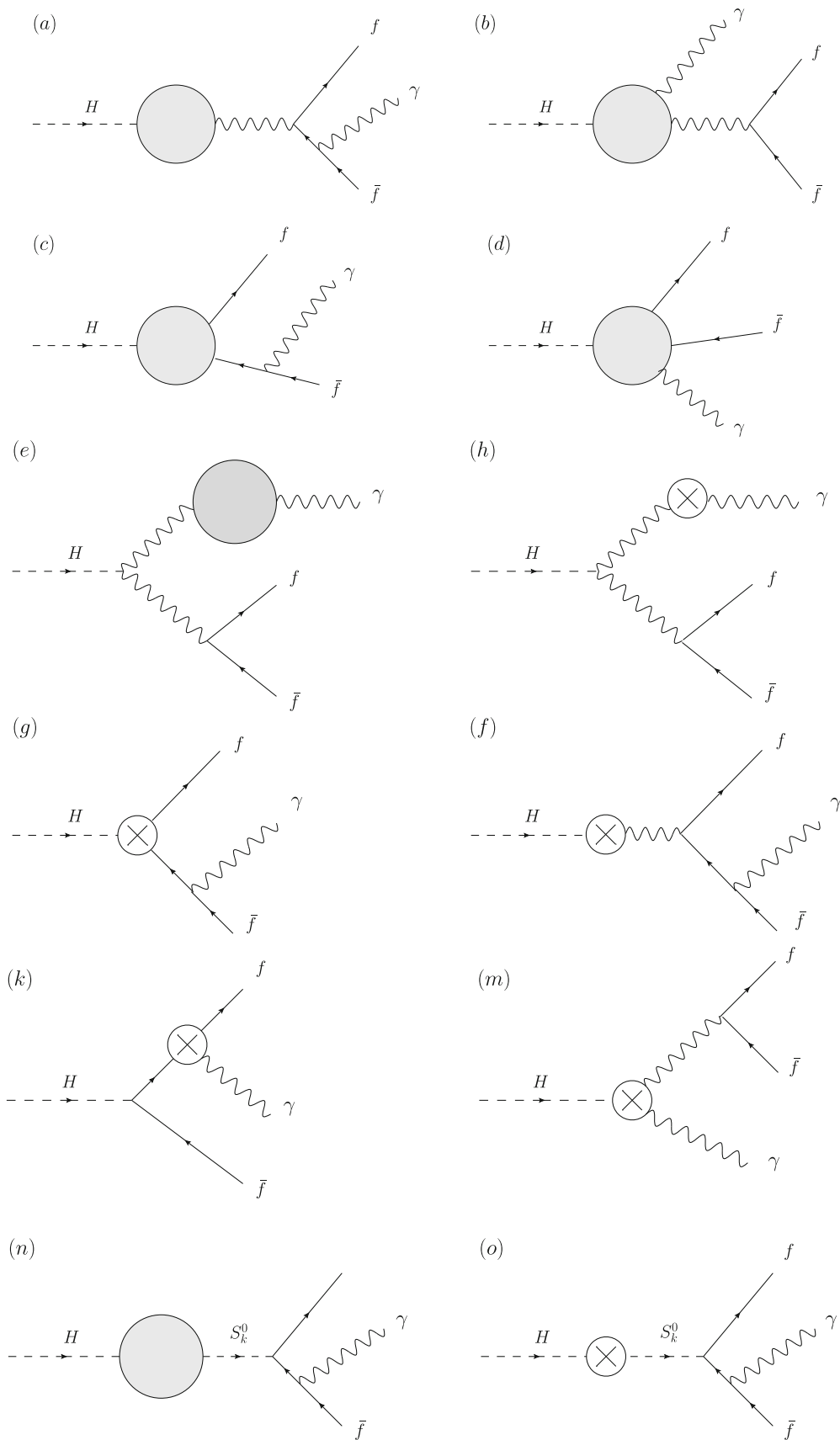


Fig. 1 Types of Feynman diagrams contributing to the SM-like Higgs decays $H \rightarrow f \bar{f} \gamma$

the general case of additional neutral gauge bosons in the loop diagrams. Their mixing is also included. In this paper, we take only $m_f \rightarrow 0$ for external fermions. For fermions at internal lines, their masses will be non-zero. Therefore, there are no infrared (IR) divergences the current calculations.

The general one-loop amplitude which obeys the Lorentz-invariant structure can be decomposed as follows [20]:

$$\mathcal{A}_{\text{loop}} = \sum_{k=1}^2 \left\{ [q_3^\mu q_k^\nu - g^{\mu\nu} q_3 \cdot q_k] \bar{u}(q_1) (F_{k,R} \gamma_\mu P_R + F_{k,L} \gamma_\mu P_L) v(q_2) \right\} \varepsilon_\nu^*(q_3), \tag{10}$$

where the Dirac spinors $\bar{u}(q_1)$, $v(q_2)$ for the external fermions and the polarization vector $\varepsilon_\nu^*(q_3)$ for the external photon are taken into account in this equation. All form factors are computed as follows:

$$F_{k,L/R} = F_{k,L/R}^{V_k^{0*}\text{-poles}} + F_{k,L/R}^{\text{Non-}V_k^{0*}} \tag{11}$$

for $k = 1, 2$. Kinematic invariant variables involved in the decay processes are taken into account: $q^2 = q_{12} = (q_1 + q_2)^2$, $q_{13} = (q_1 + q_3)^2$ and $q_{23} = (q_2 + q_3)^2$.

We first write down all Feynman amplitudes for the above diagrams. With the help of `Package-X` [47], all Dirac traces and Lorentz contractions are handled. In this computation, dimensional regularization is performed in space-time dimensions $d = 4 - 2\varepsilon$. Therefore, the trace and contractions are applied for Feynman loop momentum in general d dimensions. Subsequently, the amplitudes are then written in terms of tensor one-loop integrals. By following tensor reduction for one-loop integrals in [48] (the relevant tensor reduction formulas are shown in appendix A), all tensor one-loop integrals are expressed in terms of PV-functions. We then take $d \rightarrow 4$ for the final results. By using `LoopTools`, these scalar functions can be evaluated numerically. We then get numerical results for the decay rates.

3.1 V_k^{0*} pole contributions

In this subsection, we first arrive at the V_k^{0*} pole contributions which are corresponding to the diagram *b*. In this group of Feynman diagrams, it is easy to confirm that the form factors follow the below relation:

$$F_{k,L/R}^{V_k^{0*}\text{-poles}} = F_{1,L/R}^{V_k^{0*}\text{-poles}} = F_{2,L/R}^{V_k^{0*}\text{-poles}} \tag{12}$$

Their analytic results will be shown in the following subsections. All possible particles exchanging in the loop diagrams are included. We emphasize that analytic expressions for the form factors presented in this subsection cover the results in Ref. [49]. It means that we can reduce to the results for $H \rightarrow \nu_l \bar{\nu}_l \gamma$ of Ref. [49] by setting f to ν_l and replacing the corresponding couplings. Furthermore, all analytic formulas shown in the following subsection cover all cases of V_k^{0*}

poles. For instance, when $V_k^{0*} \rightarrow \gamma^*$, we then set $M_{V_k^0} = 0$, $\Gamma_{V_k^0} = 0$. In addition to that V_k^{0*} becomes Z (or Z') boson, we should fix $M_{V_k^0} = M_Z$ and $\Gamma_{V_k^0} = \Gamma_Z$ (or Z') respectively. In the following results, Q_V denotes the electric charge of the gauge bosons V_i , V_j and Q_S (and Q_f) is the charge of the charged Higgs bosons S_i , S_j (and fermions f).

We begin with one-loop triangle Feynman diagrams where all particles in the loop are vector bosons $V_{i,j}$ (see Fig. 2). One-loop form factors of this group of Feynman diagrams are expressed in terms of the PV functions as follows:

$$\begin{aligned} F_{k,L}^{V_k^{0*}\text{-poles}}|_{V_i, V_j} &= \frac{e Q_V}{16\pi^2} \sum_{V_i, V_j, V_k^0} \\ &\times \frac{g_{HV_i V_j} g_{V_k^0 ff}^L}{M_{V_i}^2 M_{V_j}^2 (q^2 - M_{V_k^0}^2 + i\Gamma_{V_k^0} M_{V_k^0})} \\ &\times \left\{ \left[2g_{V_k^0 AV_i V_j} (M_H^2 - M_{V_j}^2) \right. \right. \\ &+ g_{V_k^0 V_i V_j} (M_H^2 + M_{V_i}^2 + M_{V_j}^2) \left. \right] \\ &\times B_{11}(M_H^2, M_{V_i}^2, M_{V_j}^2) \\ &+ \left[g_{V_k^0 V_i V_j} (M_H^2 + 3M_{V_i}^2 - M_{V_j}^2) \right. \\ &- 2g_{V_k^0 AV_i V_j} M_{V_i}^2 \left. \right] B_1(M_H^2, M_{V_i}^2, M_{V_j}^2) \\ &+ 2M_{V_i}^2 (g_{V_k^0 V_i V_j} - g_{V_k^0 AV_i V_j}) \\ &\times B_0(M_H^2, M_{V_i}^2, M_{V_j}^2) \\ &+ 2g_{V_k^0 AV_i V_j} \left[M_H^2 B_{111} + B_{00} + 2B_{001} \right] \\ &\times (M_H^2, M_{V_i}^2, M_{V_j}^2) \\ &+ 4g_{V_k^0 V_i V_j} M_{V_i}^2 (M_{V_i}^2 + 3M_{V_j}^2 - q^2) \\ &\times C_0(0, q^2, M_H^2, M_{V_i}^2, M_{V_i}^2, M_{V_j}^2) \\ &+ 2g_{V_k^0 V_i V_j} \left[M_H^2 (M_{V_i}^2 + M_{V_j}^2 - q^2) \right. \\ &+ M_{V_i}^4 + M_{V_j}^4 + (4d - 6)M_{V_i}^2 M_{V_j}^2 \\ &- q^2 (M_{V_i}^2 + M_{V_j}^2) \left. \right] (C_{22} + C_{12}) \\ &\times (0, q^2, M_H^2, M_{V_i}^2, M_{V_i}^2, M_{V_j}^2) \\ &+ 2g_{V_k^0 V_i V_j} \left[M_H^2 (M_{V_i}^2 + M_{V_j}^2 - q^2) \right. \\ &+ 3M_{V_i}^4 - M_{V_j}^4 + (4d - 6)M_{V_i}^2 M_{V_j}^2 \\ &- q^2 (3M_{V_i}^2 - M_{V_j}^2) \left. \right] \\ &\times C_2(0, q^2, M_H^2, M_{V_i}^2, M_{V_i}^2, M_{V_j}^2) \left. \right\}, \\ F_{k,R}^{V_k^{0*}\text{-poles}}|_{V_i, V_j} &= F_{k,L}^{V_k^{0*}\text{-poles}}|_{V_i, V_j} (g_{V_k^0 ff}^L \rightarrow g_{V_k^0 ff}^R). \tag{13} \end{aligned}$$

Fig. 2 One-loop triangle diagrams with vector bosons $V_{i,j}$ in the loop

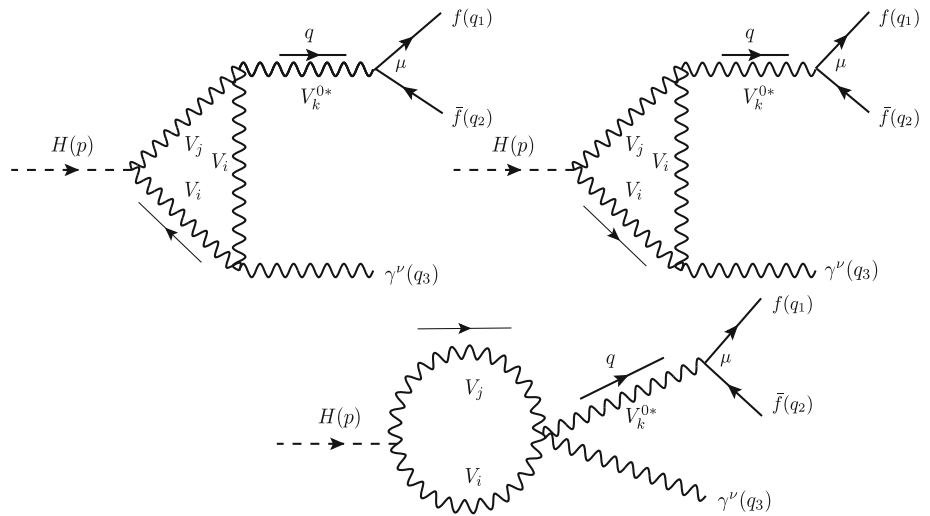
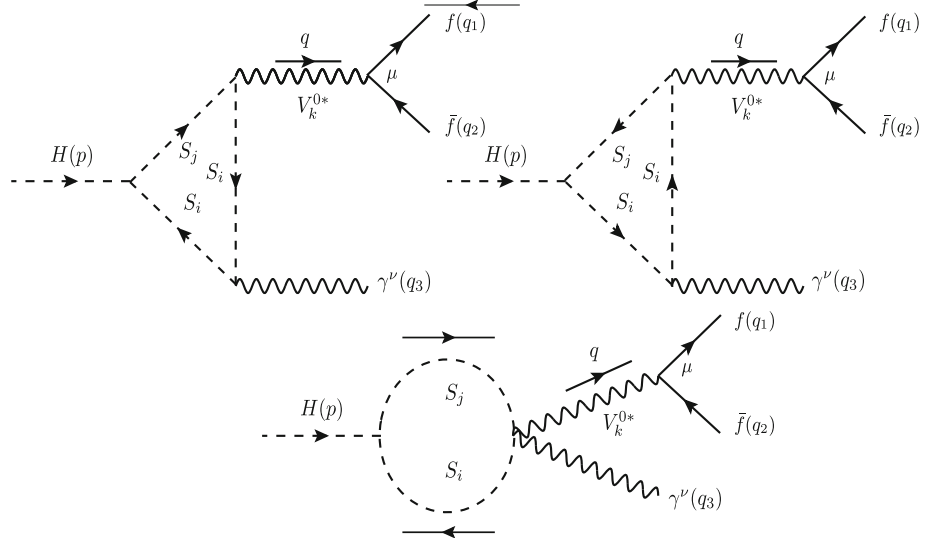


Fig. 3 One-loop triangle diagrams with scalar bosons $S_{i,j}$ in loop



The results are written in terms of B - and C -functions. We note that individual one-loop amplitudes for the diagrams in Fig. 2 can contain one-loop three-point tensor integrals up to rank $R = 6$. However, after taking into account two triangle diagrams, the amplitude for this subset of Feynman diagrams is only expressed in terms of the C -tensor integrals up to rank $R = 2$. As a result, we have up to C_{22} -functions contributing to the form factors. Furthermore, some of them may contain UV divergences but after summing all these functions, the final results are finite. The topic will be discussed at the end of this section.

We next concern one-loop triangle Feynman diagrams with S_i, S_j in the loop (as described in Fig. 3). The corresponding one-loop form factors are given:

$$F_{k,L}^{V_k^{0*}\text{-poles}}|_{S_i,S_j} = \frac{eQ_S}{4\pi^2} \times \sum_{S_i,S_j,V_k^0} \frac{g_{HS_iS_j} g_{V_k^0 S_i S_j} g_{V_k^0 ff}^L}{M_H^2 q^2 (M_H^2 - q^2) (q^2 - M_{V_k^0}^2 + i\Gamma_{V_k^0} M_{V_k^0})}$$

$$\times \left\{ (q^2 - M_H^2) [A_0(M_{S_i}^2) - A_0(M_{S_j}^2)] + M_H^2 (M_{S_i}^2 - M_{S_j}^2 - q^2) B_0(q^2, M_{S_i}^2, M_{S_j}^2) + q^2 (M_H^2 - M_{S_i}^2 + M_{S_j}^2) B_0(M_H^2, M_{S_i}^2, M_{S_j}^2) + 2M_H^2 q^2 (M_H^2 - q^2) C_{12}(0, q^2, M_H^2, M_{S_i}^2, M_{S_j}^2, M_{S_j}^2) \right\},$$

$$F_{k,R}^{V_k^{0*}\text{-poles}}|_{S_i,S_j} = F_{k,L}^{V_k^{0*}\text{-poles}}|_{S_i,S_j} (g_{V_k^0 ff}^L \rightarrow g_{V_k^0 ff}^R). \tag{14}$$

We observe the factor $1/(M_H^2 - q^2)$ in these formulas. This may lead to the kinematic divergence in the limit of $q^2 \rightarrow M_H^2$. However, we check that this divergence will be cancelled out. In the limit of $q^2 \rightarrow M_H^2$, the sum of B_0 -terms in these formulas is vanishing. Other terms contain the overall factor $M_H^2 - q^2$ that is also cancelled out the pole $1/(M_H^2 - q^2)$. As a result, the final results stay finite in the limit of $q^2 \rightarrow M_H^2$.

Fig. 4 One-loop triangle diagrams with two scalar bosons S_i and a vector boson V_j in the loop

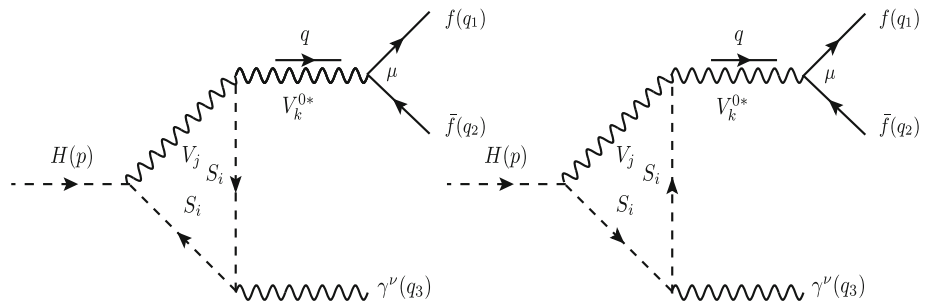
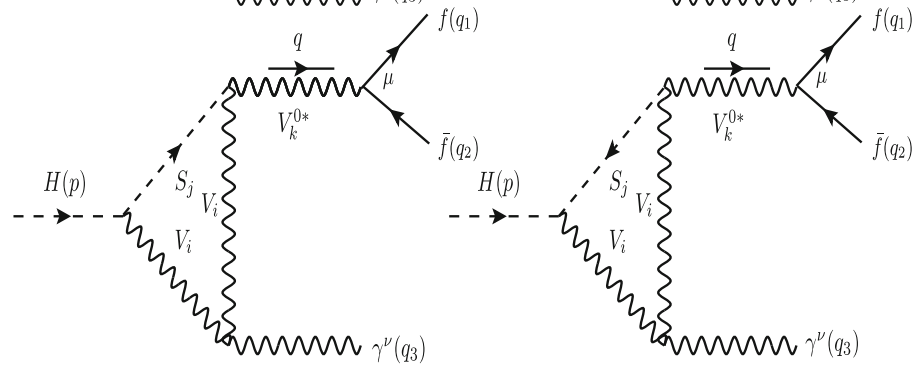


Fig. 5 One-loop triangle diagrams with a scalar boson S_j and two vector bosons V_i in the loop



Similarly, we have the contributions of one-loop triangle Feynman diagrams with exchanging scalar boson S_i and vector boson V_j in the loop. The Feynman diagrams are depicted in Fig. 4. Applying the same procedure, one has the form factors

$$\begin{aligned}
 F_{k,L}^{V_k^{0*}\text{-poles}}|_{S_i,V_j} &= \frac{eQ_V}{8\pi^2} \\
 &\times \sum_{S_i,V_j,V_k^0} \frac{g_{HS_iV_j} g_{V_k^0 S_i V_j} g_{V_k^0 ff}^L}{M_H^2 M_{V_j}^2 q^2 (q^2 - M_H^2) (q^2 - M_{V_k^0}^2 + i\Gamma_{V_k^0} M_{V_k^0})} \\
 &\times \left\{ (q^2 - M_H^2) (M_H^2 - M_{S_i}^2 + M_{V_j}^2) [A_0(M_{S_i}^2) - A_0(M_{V_j}^2)] \right. \\
 &+ M_H^2 [q^2 (M_{S_i}^2 + 3M_{V_j}^2 - M_H^2) \\
 &+ (M_{S_i}^2 - M_{V_j}^2) (M_H^2 - M_{S_i}^2 + M_{V_j}^2)] B_0(q^2, M_{S_i}^2, M_{V_j}^2) \\
 &+ q^2 [M_H^2 - (M_{S_i} + M_{V_j})^2] \\
 &\times [M_H^2 - (M_{S_i} - M_{V_j})^2] B_0(M_H^2, M_{S_i}^2, M_{V_j}^2) \\
 &+ 2M_H^2 q^2 (M_H^2 - q^2) (M_H^2 - M_{S_i}^2 + M_{V_j}^2) \\
 &\left. \times C_{12}(0, q^2, M_H^2, M_{S_i}^2, M_{V_j}^2) \right\}, \\
 F_{k,R}^{V_k^{0*}\text{-poles}}|_{S_i,V_j} &= F_{k,L}^{V_k^{0*}\text{-poles}}|_{S_i,V_j} (g_{V_k^0 ff}^L \rightarrow g_{V_k^0 ff}^R). \tag{15}
 \end{aligned}$$

We also consider the contributions of one-loop triangle diagrams with exchanging a scalar boson S_j and two vector bosons V_i in the loop. The Feynman diagrams are presented in Fig. 5. The corresponding form factors for the above diagrams are given:

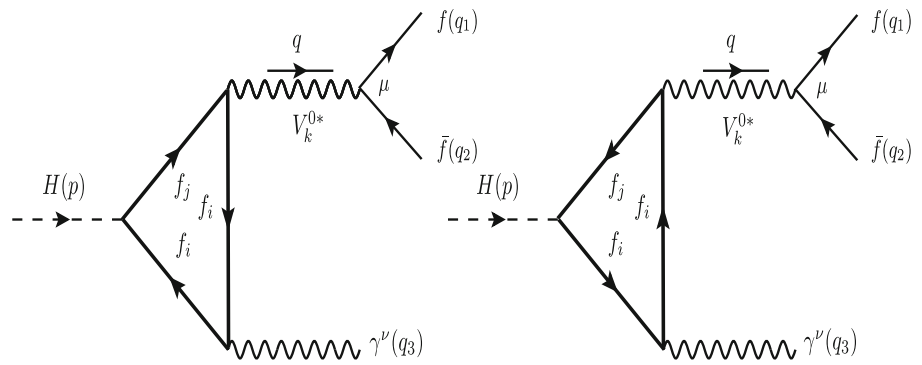
$$F_{k,L}^{V_k^{0*}\text{-poles}}|_{V_i,S_j} = \frac{eQ_V}{8\pi^2}$$

$$\begin{aligned}
 &\times \sum_{V_i,S_j,V_k^0} \frac{g_{HV_i S_j} g_{V_k^0 V_i S_j} g_{V_k^0 ff}^L}{M_H^2 M_{V_i}^2 q^2 (M_H^2 - q^2) (q^2 - M_{V_k^0}^2 + i\Gamma_{V_k^0} M_{V_k^0})} \\
 &\times \left\{ (M_H^2 - q^2) (M_H^2 - M_{S_j}^2 + M_{V_i}^2) [A_0(M_{S_j}^2) - A_0(M_{V_i}^2)] \right. \\
 &+ q^2 [M_H^2 (M_H^2 + 4M_{V_i}^2) - (M_{S_j}^2 - M_{V_i}^2)^2] B_0(M_H^2, M_{V_i}^2, M_{S_j}^2) \\
 &- M_H^2 [M_H^2 (M_{S_j}^2 - M_{V_i}^2 + q^2) + M_{S_j}^2 (2M_{V_i}^2 - M_{S_j}^2 - q^2) \\
 &+ M_{V_i}^2 (5q^2 - M_{V_i}^2)] B_0(q^2, M_{V_i}^2, M_{S_j}^2) \\
 &+ 2M_H^2 q^2 (M_H^2 - q^2) (M_H^2 - M_{S_j}^2 + M_{V_i}^2) \\
 &C_{12}(0, q^2, M_H^2, M_{V_i}^2, M_{S_j}^2) \\
 &+ 4M_H^2 M_{V_i}^2 q^2 (M_H^2 - q^2) C_0(0, q^2, M_H^2, M_{V_i}^2, M_{V_i}^2, M_{S_j}^2) \left. \right\}, \\
 F_{k,R}^{V_k^{0*}\text{-poles}}|_{V_i,S_j} &= F_{k,L}^{V_k^{0*}\text{-poles}}|_{V_i,S_j} (g_{V_k^0 ff}^L \rightarrow g_{V_k^0 ff}^R). \tag{16}
 \end{aligned}$$

Finally, we have to consider fermions exchanging in the one-loop triangle diagrams (shown in Fig. 6). The form factors then read

$$\begin{aligned}
 F_{k,L}^{V_k^{0*}\text{-poles}}|_{f_i,f_j} &= \frac{eQ_f}{4\pi^2} \\
 &\times \sum_{f_i,f_j,V_k^0} \frac{N_C^f g_{V_k^0 ff}^L}{(q^2 - M_{V_k^0}^2 + i\Gamma_{V_k^0} M_{V_k^0})} \\
 &\times \left\{ [2m_{f_i} (g_{Hf_i f_j}^L g_{V_k^0 f_i f_j}^L + g_{Hf_i f_j}^R g_{V_k^0 f_i f_j}^R) \right. \\
 &+ 2m_{f_j} (g_{Hf_i f_j}^L g_{V_k^0 f_i f_j}^R + g_{Hf_i f_j}^R g_{V_k^0 f_i f_j}^L)] \\
 &\left. \times [C_{22} + C_{12}](0, q^2, M_H^2, m_{f_i}^2, m_{f_i}^2, m_{f_j}^2) \right\}
 \end{aligned}$$

Fig. 6 One-loop triangle diagrams with charged fermions $f_{i,j}$ in the loop



$$\begin{aligned}
 & + \left[3m_{f_i} (g_{Hf_i f_j}^L g_{V_k^0 f_i f_j}^L + g_{Hf_i f_j}^R g_{V_k^0 f_i f_j}^R) \right. \\
 & + m_{f_j} (g_{Hf_i f_j}^L g_{V_k^0 f_i f_j}^R + g_{Hf_i f_j}^R g_{V_k^0 f_i f_j}^L) \left. \right] \\
 & \times C_2(0, q^2, M_H^2, m_{f_i}^2, m_{f_j}^2, m_{f_j}^2) \\
 & + m_{f_i} (g_{Hf_i f_j}^L g_{V_k^0 f_i f_j}^R \\
 & + g_{Hf_i f_j}^R g_{V_k^0 f_i f_j}^L) C_0(0, q^2, M_H^2, m_{f_i}^2, m_{f_j}^2, m_{f_j}^2) \Big\}, \\
 & F_{k,R}^{V_k^{0*}\text{-poles}}|_{f_i, f_j} \\
 & = F_{k,L}^{V_k^{0*}\text{-poles}}|_{f_i, f_j} (g_{V_k^0 f f}^L \rightarrow g_{V_k^0 f f}^R). \tag{17}
 \end{aligned}$$

3.2 Non- V_k^{0*} pole contributions

We turn our attention to the non- V_k^{0*} pole contributions, considering all possible particles exchanging in the loop diagrams ($c + d$). One first arrives at the group of Feynman diagrams with vector bosons $V_{i,j}$ at internal lines (as depicted in Fig. 7). Analytic formulas for the form factors are given:

$$\begin{aligned}
 F_{1,L}^{\text{Non-}V_k^{0*}}|_{V_i, V_j} &= \frac{eQ_V}{16\pi^2} \\
 & \times \sum_{V_i, V_j} \frac{g_{HV_i V_j} g_{V_i f v_f}^L g_{V_j f v_f}^L}{M_{V_i}^2 M_{V_j}^2} \\
 & \times \left\{ -2M_{V_i}^2 \left[C_0(0, q_{12}, M_H^2, M_{V_i}^2, M_{V_i}^2, M_{V_j}^2) \right. \right. \\
 & + C_0(q_{12}, 0, M_H^2, M_{V_i}^2, M_{V_j}^2, M_{V_j}^2) \left. \right] \\
 & - (M_H^2 + M_{V_i}^2 + M_{V_j}^2) \left\{ [C_{22} + C_{12}] \right. \\
 & (0, q_{12}, M_H^2, M_{V_i}^2, M_{V_i}^2, M_{V_j}^2) \\
 & + [C_{22} + C_{12}] (q_{12}, 0, M_H^2, M_{V_i}^2, M_{V_j}^2, M_{V_j}^2) \left. \right\} \\
 & - (M_H^2 + 3M_{V_i}^2 - M_{V_j}^2) \left[C_2(0, q_{12}, M_H^2, \right. \\
 & M_{V_i}^2, M_{V_i}^2, M_{V_j}^2) \\
 & \left. + C_2(q_{12}, 0, M_H^2, M_{V_i}^2, M_{V_j}^2, M_{V_j}^2) \right]
 \end{aligned}$$

$$\begin{aligned}
 & + 2(M_{V_j}^2 - M_{V_i}^2) C_1(q_{12}, 0, M_H^2, M_{V_i}^2, M_{V_j}^2, M_{V_j}^2) \\
 & + (8 - 2d) M_{V_i}^2 M_{V_j}^2 \left[D_3(0, 0, 0, M_H^2; \right. \\
 & q_{12}, q_{13}, M_{V_i}^2, 0, M_{V_j}^2, M_{V_j}^2) \\
 & + D_3(0, 0, 0, M_H^2; q_{23}, q_{12}, M_{V_i}^2, M_{V_i}^2, 0, M_{V_j}^2) \left. \right] \\
 & + (4 - 2d) M_{V_i}^2 M_{V_j}^2 \left\{ [D_{33} + D_{23} + D_{13}] \right. \\
 & (0, 0, 0, M_H^2; q_{23}, q_{12}, M_{V_i}^2, M_{V_i}^2, 0, M_{V_j}^2) \\
 & + [D_{33} + D_{23}] (0, 0, 0, M_H^2; q_{12}, q_{13}, \\
 & M_{V_i}^2, 0, M_{V_j}^2, M_{V_j}^2) \left. \right\} \\
 & + 4M_{V_i}^2 M_{V_j}^2 D_2(0, 0, 0, M_H^2; q_{12}, q_{13}, \\
 & M_{V_i}^2, 0, M_{V_j}^2, M_{V_j}^2) \Big\}, \tag{18}
 \end{aligned}$$

$$\begin{aligned}
 F_{1,R}^{\text{Non-}V_k^{0*}}|_{V_i, V_j} &= F_{1,L}^{\text{Non-}V_k^{0*}}|_{V_i, V_j} \\
 & (g_{V_i f v_f}^L \rightarrow g_{V_i f v_f}^R; g_{V_j f v_f}^L \rightarrow g_{V_j f v_f}^R), \tag{19}
 \end{aligned}$$

$$\begin{aligned}
 F_{2,L}^{\text{Non-}V_k^{0*}}|_{V_i, V_j} &= F_{1,L}^{\text{Non-}V_k^{0*}}|_{V_i, V_j} \\
 & (\{q_{13}, q_{23}\} \rightarrow \{q_{23}, q_{13}\}), \tag{20}
 \end{aligned}$$

$$\begin{aligned}
 F_{2,R}^{\text{Non-}V_k^{0*}}|_{V_i, V_j} &= F_{2,L}^{\text{Non-}V_k^{0*}}|_{V_i, V_j} \\
 & (g_{V_i f v_f}^L \rightarrow g_{V_i f v_f}^R; g_{V_j f v_f}^L \rightarrow g_{V_j f v_f}^R). \tag{21}
 \end{aligned}$$

We find that the result is presented in terms of C - and D -functions up to C_{22} - (D_{33} -) coefficients. The reason for this fact is explained as follows. Due to the exchange of vector bosons in the loop, we have to handle one-loop tensor integrals with rank $R \geq 3$ in the amplitude of individual diagrams. However, they are cancelled out after summing all diagrams. As a result, the total amplitude is only expressed in terms of tensor integrals with $R \leq 2$ that explain for the above result.

For neutral vector bosons V_i^0, V_j^0 at internal lines (see Fig. 8), the corresponding form factors are obtained as

$$F_{1,L}^{\text{Non-}V_k^{0*}}|_{V_i^0, V_j^0} = \frac{eQ_f}{16\pi^2}$$

Fig. 7 One-loop triangle and box diagrams with bosons $V_{i,j}$ in the loop

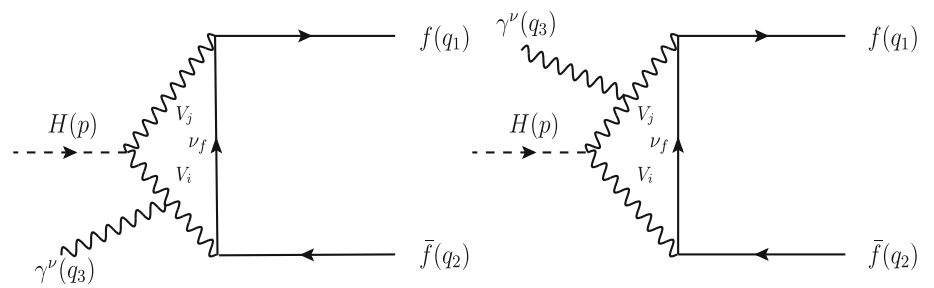


Fig. 8 One-loop triangle and box diagrams with vector bosons V_i^0, V_j^0 in the loop

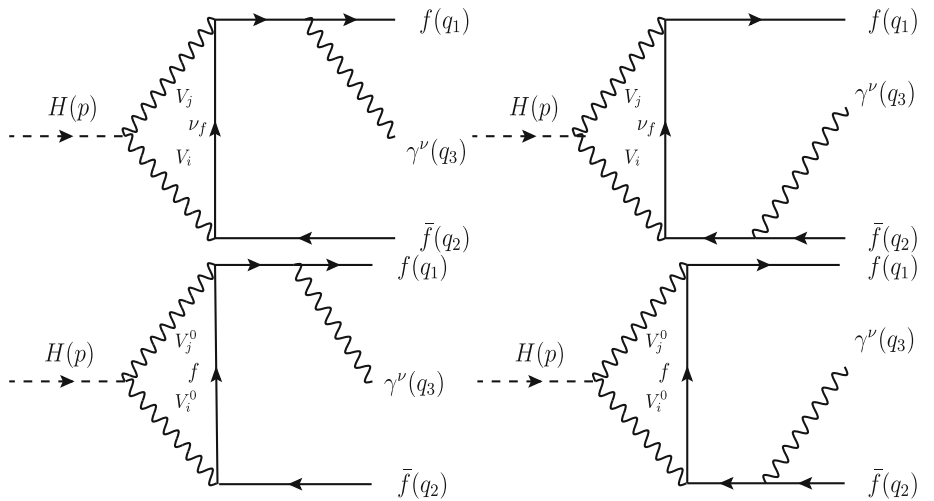


Fig. 9 One-loop diagrams with charged scalar bosons $S_{i,j}$ in the loop

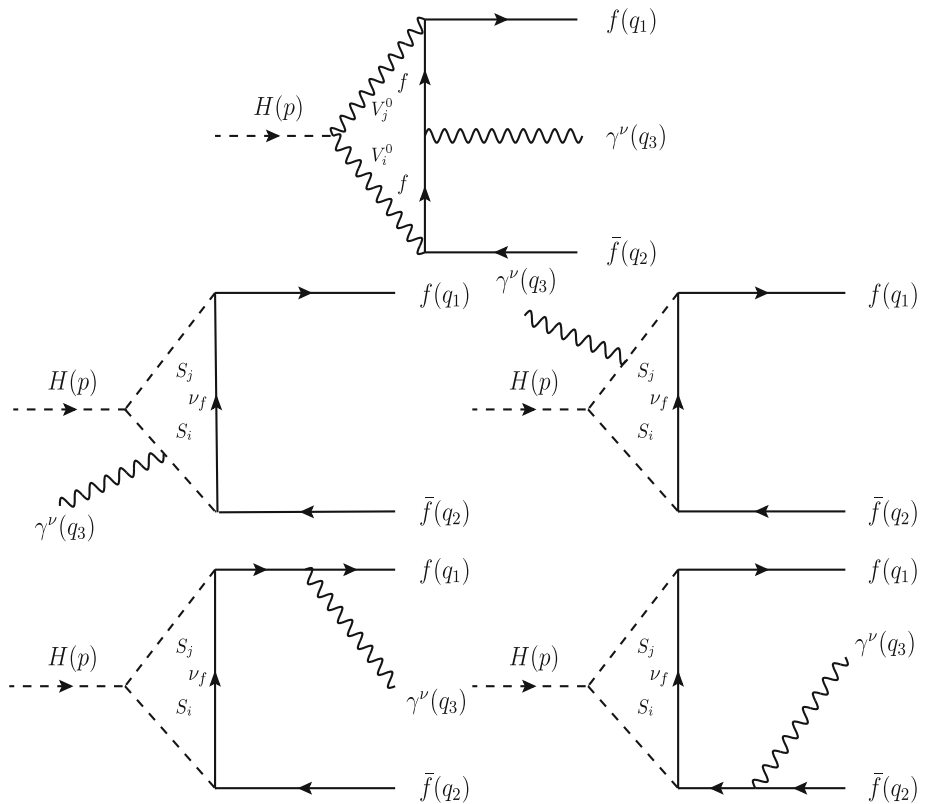


Fig. 10 One-loop box diagrams with neutral scalar bosons $S_{i,j}^0$ particles in loop

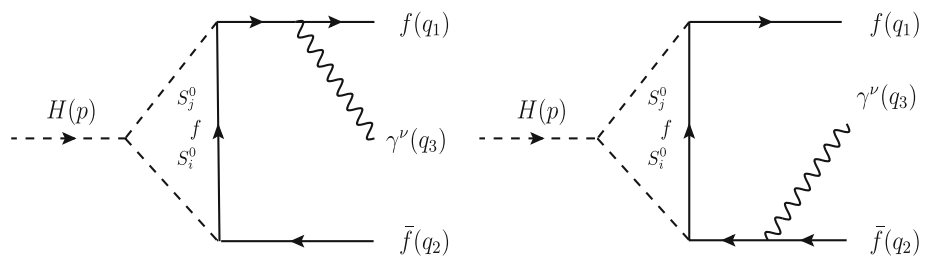


Fig. 11 One-loop diagrams with exchanging vector boson V_i and scalar boson S_j particles in loop

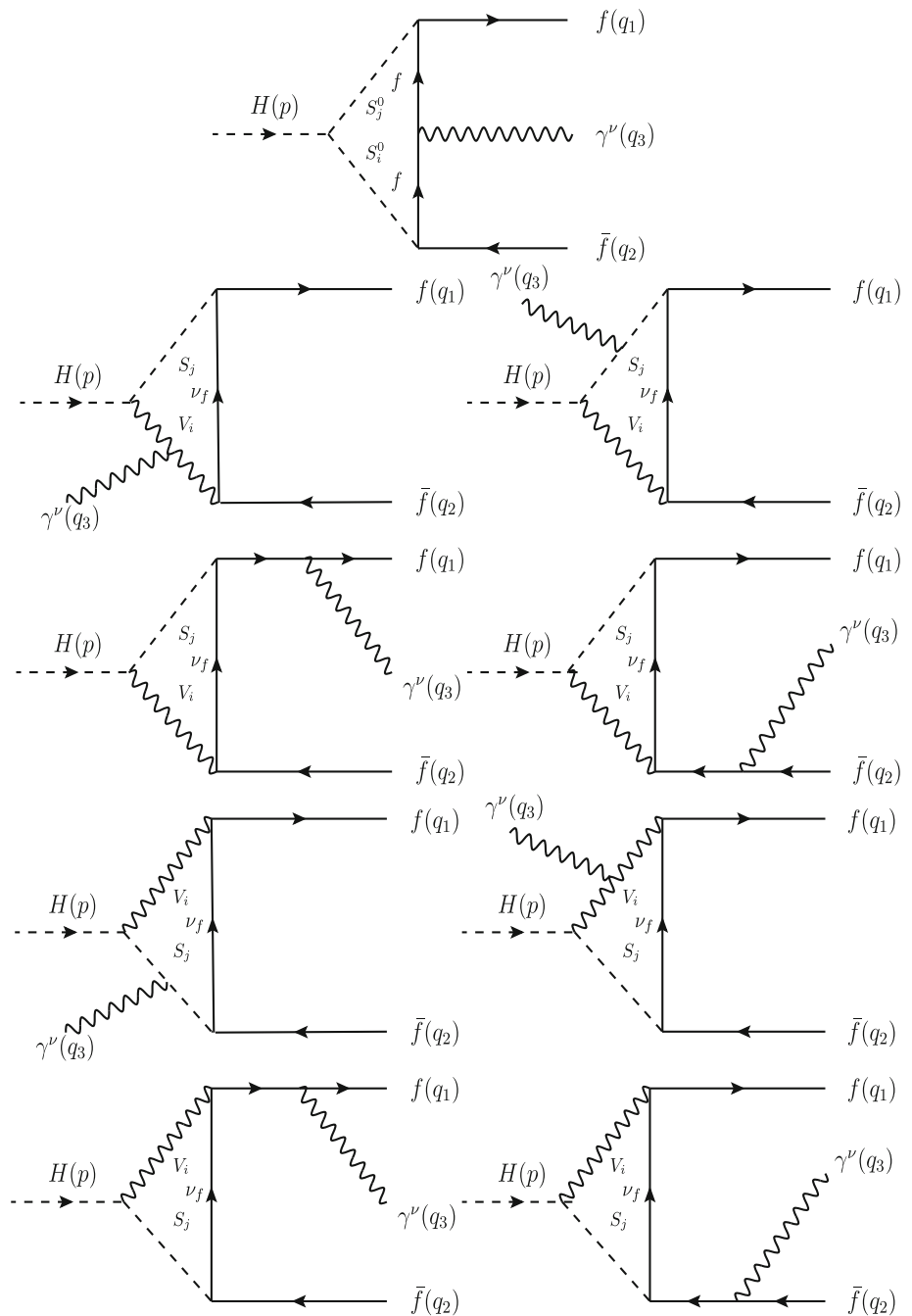
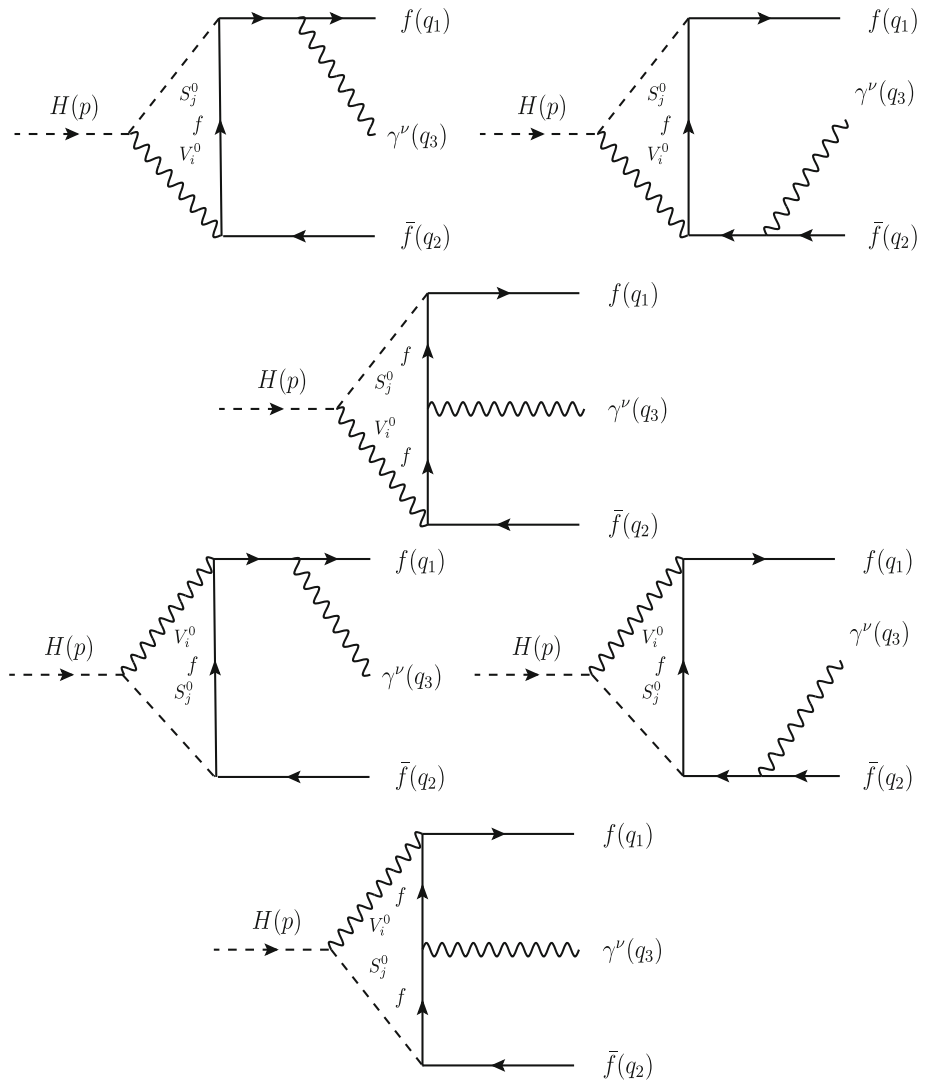


Fig. 12 One-loop diagrams with vector boson V_i^0 and scalar boson S_j^0 in the loop



$$\begin{aligned} &\times \sum_{V_i^0, V_j^0} g_{H V_i^0 V_j^0} g_{V_i^0 f f}^L g_{V_j^0 f f}^L \\ &\times \left\{ (4 - 2d)[D_{33} + D_{23}] + (8 - 2d)D_3 \right\} \\ &(0, 0, 0, M_H^2, q_{23}, q_{13}, M_{V_i^0}^2, 0, 0, M_{V_j^0}^2), \end{aligned} \tag{22}$$

$$\begin{aligned} F_{1,R}^{\text{Non-}V_k^{0*}} |_{V_i^0, V_j^0} &= F_{1,L}^{\text{Non-}V_k^{0*}} |_{V_i^0, V_j^0} \\ &\left(g_{V_i^0 f f}^L \rightarrow g_{V_i^0 f f}^R; g_{V_j^0 f f}^L \rightarrow g_{V_j^0 f f}^R \right), \end{aligned} \tag{23}$$

$$\begin{aligned} F_{2,L}^{\text{Non-}V_k^{0*}} |_{V_i^0, V_j^0} &= F_{1,L}^{\text{Non-}V_k^{0*}} |_{V_i^0, V_j^0} \\ &\left(\{q_{13}, q_{23}\} \rightarrow \{q_{23}, q_{13}\} \right), \end{aligned} \tag{24}$$

$$\begin{aligned} F_{2,R}^{\text{Non-}V_k^{0*}} |_{V_i^0, V_j^0} &= F_{2,L}^{\text{Non-}V_k^{0*}} |_{V_i^0, V_j^0} \\ &\left(g_{V_i^0 f f}^L \rightarrow g_{V_i^0 f f}^R; g_{V_j^0 f f}^L \rightarrow g_{V_j^0 f f}^R \right). \end{aligned} \tag{25}$$

Next, we also consider one-loop diagrams with charged scalar bosons $S_{i,j}$ at internal lines (shown in Fig. 9). The

results read

$$\begin{aligned} F_{1,L}^{\text{Non-}V_k^{0*}} |_{S_i, S_j} &= \frac{e Q_S}{8\pi^2} \\ &\times \sum_{S_i, S_j} g_{H S_i S_j} g_{S_i f v_f}^R g_{S_j f v_f}^R \\ &\times \left\{ \left[D_{33} + D_{23} + D_3 \right] \right. \\ &\times (0, 0, 0, M_H^2; q_{12}, q_{13}, M_{S_i}^2, 0, M_{S_j}^2, M_{S_j}^2) \\ &+ \left[D_{33} + D_{23} + D_{13} + D_3 \right] \\ &\left. \times (0, 0, 0, M_H^2; q_{23}, q_{12}, M_{S_i}^2, M_{S_i}^2, 0, M_{S_j}^2) \right\}, \end{aligned} \tag{26}$$

$$\begin{aligned} F_{1,R}^{\text{Non-}V_k^{0*}} |_{S_i, S_j} &= F_{1,L}^{\text{Non-}V_k^{0*}} |_{S_i, S_j} \\ &\left(g_{S_i f v_f}^R \rightarrow g_{S_i f v_f}^L; g_{S_j f v_f}^R \rightarrow g_{S_j f v_f}^L \right), \end{aligned} \tag{27}$$

$$F_{2,L}^{\text{Non-}V_k^{0*}} |_{S_i, S_j} = F_{1,L}^{\text{Non-}V_k^{0*}} |_{S_i, S_j}$$

$$\left(\{q_{13}, q_{23}\} \rightarrow \{q_{23}, q_{13}\} \right), \tag{28}$$

$$F_{2,R}^{\text{Non-}V_k^{0*}}|_{S_i, S_j} = F_{2,L}^{\text{Non-}V_k^{0*}}|_{S_i, S_j} \left(g_{S_i f v_f}^R \rightarrow g_{S_i f v_f}^L; g_{S_j f v_f}^R \rightarrow g_{S_j f v_f}^L \right). \tag{29}$$

Furthermore, one also has the contributions of neutral scalar bosons $S_{i,j}^0$ exchanging in the loop diagrams (as described in Fig. 10). Analytic results for the form factors then read

$$F_{1,L}^{\text{Non-}V_k^{0*}}|_{S_i^0, S_j^0} = -\frac{eQ_f}{8\pi^2} \times \sum_{S_i^0, S_j^0} g_H S_i^0 S_j^0 g_{S_i^0 f f}^L g_{S_j^0 f f}^R \times [D_{33} + D_{23} + D_3] \times (0, 0, 0, M_H^2; q_{23}, q_{13}; M_{S_i^0}^2, 0, 0, M_{S_j^0}^2), \tag{30}$$

$$F_{1,R}^{\text{Non-}V_k^{0*}}|_{S_i^0, S_j^0} = F_{1,L}^{\text{Non-}V_k^{0*}}|_{S_i^0, S_j^0} \left(g_{S_i^0 f f}^L \rightarrow g_{S_i^0 f f}^R; g_{S_j^0 f f}^R \rightarrow g_{S_j^0 f f}^L \right), \tag{31}$$

$$F_{2,L}^{\text{Non-}V_k^{0*}}|_{S_i^0, S_j^0} = F_{1,L}^{\text{Non-}V_k^{0*}}|_{S_i^0, S_j^0} \left(\{q_{13}, q_{23}\} \rightarrow \{q_{23}, q_{13}\} \right), \tag{32}$$

$$F_{2,R}^{\text{Non-}V_k^{0*}}|_{S_i^0, S_j^0} = F_{2,L}^{\text{Non-}V_k^{0*}}|_{S_i^0, S_j^0} \left(g_{S_i^0 f f}^L \rightarrow g_{S_i^0 f f}^R; g_{S_j^0 f f}^R \rightarrow g_{S_j^0 f f}^L \right). \tag{33}$$

We now consider non- V_k^{*0} pole one-loop diagrams with scalar S_j (or S_j^0) and vector V_i (or V_i^0) propagating in the loop. The diagrams are depicted in Figs. 11 and 12. The calculations are performed with the same procedure. We finally find that these contributions are proportional to m_f . As a result, in the limit of $m_f \rightarrow 0$, one confirms that

$$F_{k,L}^{\text{Non-}V_k^{0*}}|_{V_i, S_j} = F_{k,R}^{\text{Non-}V_k^{0*}}|_{V_i, S_j} = 0, \tag{34}$$

$$F_{k,L}^{\text{Non-}V_k^{0*}}|_{V_i^0, S_j^0} = F_{k,R}^{\text{Non-}V_k^{0*}}|_{V_i^0, S_j^0} = 0 \tag{35}$$

for $k = 1, 2$.

We verify the ultraviolet finiteness of the results. We find that the UV-divergent parts of all the above form factors come from all B -functions, while C - and D -functions in this paper are UV-finite. Higher rank tensor B -functions can be reduced into B_0 and A_0 . We verify that the sum of all B -functions gives a UV-finite result. As a result, all the form factors are UV-finite (see our previous paper [49] for example).

Having the correct form factors for the decay processes, the decay rate is given by [20]:

$$\frac{d\Gamma}{dq_{12}dq_{13}} = \frac{q_{12}}{512\pi^3 M_H^3} \left[q_{13}^2 (|F_{1,R}|^2 + |F_{2,R}|^2) + q_{23}^2 (|F_{1,L}|^2 + |F_{2,L}|^2) \right]. \tag{36}$$

Table 1 All the couplings involving the decay processes $H \rightarrow f \bar{f} \gamma$ in the SM

Vertices	Couplings
$g_{H V_i V_j}$	$e M_W / s_W$
$g_{V_k^0 V_i V_j}$	$e c_W / s_W$
$g_{V_k^0 A V_i V_j}$	$e^2 c_W / s_W$
$g_{V_k^L v_f v_f}$	$e / (2s_W c_W)$
$g_{V_k^R v_f v_f}$	0
$g_{H f_i f_j}^{L,R}$	$e m_f / (2s_W M_W)$
$g_{V_k^L f_i f_j}$	$e(T_3^f - Q_f s_W^2) / (s_W c_W)$
$g_{V_k^R f_i f_j}$	$-e Q_f s_W / c_W$
$g_{V_i^L f v_f}$	$e / (\sqrt{2} s_W)$
$g_{V_i^R f v_f}$	0

Integrating the above integrand over $0 \leq q_{12} \leq M_H^2$ and $0 \leq q_{13} \leq M_H^2 - q_{12}$, one gets the total decay rates. We show typical examples which we apply our analytical results for $H \rightarrow f \bar{f} \gamma$ to the SM, the $U(1)_{B-L}$ extension of the SM, THDM. Phenomenological results of these models will be presented in the next section.

4 Applications

We are going to apply the above results to the standard model, the $U(1)_{B-L}$ extension of the SM, and the THDM. For phenomenological analyses, we use the following input parameters: $\alpha = 1/137.035999084$, $M_Z = 91.1876$ GeV, $\Gamma_Z = 2.4952$ GeV, $M_W = 80.379$ GeV, $M_H = 125.1$ GeV, $m_\tau = 1.77686$ GeV, $m_t = 172.76$ GeV, $m_b = 4.18$ GeV, $m_s = 0.93$ GeV and $m_c = 1.27$ GeV. Depending on the models under consideration, the input values for new parameters are then shown.

4.1 Standard model

We first reduce our result to the case of the standard model. In this case, we have $V_i, V_j \rightarrow W^+, W^-, V_k^0 \rightarrow Z, \gamma$. All couplings relating to the decay channels $H \rightarrow f \bar{f} \gamma$ in the SM are replaced as in Table 1.

In the SM, the form factors are obtained by taking the contributions of Eqs. (13, 17, 18, 22). Using the above couplings, we then get a compact expression for the form factors as follows:

$$F_{2L} = \frac{\alpha^2 m_\tau^2}{3s_W M_W} \left[\frac{16}{q_{12}} \right]$$

Table 2 Numerical checks for form factor F_{2L} in this work with b_1 in A2 of [20]

(q_{12}, q_{13})	This work	Ref. [20]
(100, 200)	$9.62231539663501 \cdot 10^{-8}$ $-3.501515874673991 \cdot 10^{-10} i$	$9.62231539662956 \cdot 10^{-8}$ $-3.501515874674078 \cdot 10^{-10} i$
(-100, 200)	$-9.95227151085161 \cdot 10^{-8}$ $-3.531494528007124 \cdot 10^{-10} i$	$-9.95227151084899 \cdot 10^{-8}$ $-3.531494528006995 \cdot 10^{-10} i$
(100, -200)	$9.62360254230002 \cdot 10^{-8}$ $-3.597907189717628 \cdot 10^{-10} i$	$9.62360254229717 \cdot 10^{-8}$ $-3.597907189717582 \cdot 10^{-10} i$
(-100, -200)	$-9.95098785515085 \cdot 10^{-8}$ $-3.622848558573573 \cdot 10^{-10} i$	$-9.95098785514946 \cdot 10^{-8}$ $-3.622848558573332 \cdot 10^{-10} i$

$$\begin{aligned}
 & + \frac{2(8s_W^2 - 3)}{es_W c_W} \left[\frac{g_{Zff}^L}{q_{12} - M_Z^2 + i\Gamma_Z M_Z} \right] \\
 & \times \left\{ 4(C_{22} + C_{12} + C_2) + C_0 \right\} (0, q_{12}, M_H^2, m_t^2, m_t^2, m_t^2) \\
 & + \frac{\alpha^2}{s_W M_W^3} \left[\frac{1}{q_{12}} - \frac{c_W}{es_W} \frac{g_{Zff}^L}{q_{12} - M_Z^2 + i\Gamma_Z M_Z} \right] \\
 & \times \left[-M_H^2 (B_1 + 3B_{11} + 2B_{111}) - 2(B_{00} + 2B_{001}) \right] \\
 & \times (M_H^2, M_W^2, M_W^2) \\
 & + \left[4M_W^2 (q_{12} - M_H^2) + 2M_H^2 q_{12} + 8(1 - d)M_W^4 \right] \\
 & \times (C_{22} + C_{12} + C_2) (0, q_{12}, M_H^2, M_W^2, M_W^2, M_W^2) \\
 & + 4M_W^2 (q_{12} - 4M_W^2) C_0 (0, q_{12}, M_H^2, M_W^2, M_W^2, M_W^2) \left. \right\} \\
 & + \frac{\alpha}{4\pi s_W M_W^3} (g_{Wff\nu_f}^L)^2 \\
 & \times \left\{ (-M_H^2 - 2M_W^2) \left[(C_{12} \right. \right. \\
 & + C_{11} + C_1) (M_H^2, 0, q_{12}, M_W^2, M_W^2, M_W^2) \\
 & + (C_{12} + C_{11} + C_1) (M_H^2, q_{12}, 0, M_W^2, M_W^2, M_W^2) \left. \right] \\
 & - 2M_W^2 \left[C_0 (M_H^2, 0, q_{12}, M_W^2, M_W^2, M_W^2) \right. \\
 & + C_0 (M_H^2, q_{12}, 0, M_W^2, M_W^2, M_W^2) \left. \right] \\
 & + 2M_W^4 (2 - d) \left[(D_{13} + D_{12} + D_{11}) \right. \\
 & (M_H^2, 0, 0, 0; q_{12}, q_{13}, M_W^2, M_W^2, M_W^2, 0) \\
 & + (D_{23} + D_{22} + D_{13} + 2D_{12} + D_{11}) \\
 & (M_H^2, 0, 0, 0; q_{23}, q_{12}, M_W^2, M_W^2, 0, M_W^2) \left. \right] \\
 & - 4M_W^4 \left[(D_3 + D_2 + D_0) \right. \\
 & (M_H^2, 0, 0, 0; q_{12}, q_{13}, M_W^2, M_W^2, M_W^2, 0) \\
 & \left. \left. + D_0 (M_H^2, 0, 0, 0; q_{23}, q_{12}, M_W^2, M_W^2, 0, M_W^2) \right] \right\}
 \end{aligned}$$

Table 3 Cross-check the results of the decay widths in this work with [13]

k	This work	Ref. [13]
0	0.576865	0.5782
0.1	0.242514	0.245
0.2	0.184121	0.1897
0.3	0.121368	0.1242
0.4	0.0572478	0.05844

$$\begin{aligned}
 & -2dM_W^4 \left[(D_2 + D_1) \right. \\
 & (M_H^2, 0, 0, 0; q_{23}, q_{12}, M_W^2, M_W^2, 0, M_W^2) \\
 & \left. + D_1 (M_H^2, 0, 0, 0; q_{12}, q_{13}, M_W^2, M_W^2, M_W^2, 0) \right] \left. \right\} \\
 & + \frac{\alpha M_W}{2\pi c_W^2 s_W} (g_{Zff}^L)^2 \left\{ (d - 2) \right. \\
 & \times \left[D_{23} + D_{22} + D_{13} + 2D_{12} + D_{11} \right] \\
 & (M_H^2, 0, 0, 0; q_{23}, q_{13}, M_Z^2, M_Z^2, 0, 0) \\
 & \left. + \left[d(D_2 + D_1) + 2(D_3 + D_0) \right] \right. \\
 & \left. (M_H^2, 0, 0, 0; q_{23}, q_{13}, M_Z^2, M_Z^2, 0, 0) \right\}, \tag{37}
 \end{aligned}$$

where some coupling constants relate in this representation like $g_{Wff\nu_f}^L = e/(\sqrt{2}s_W)$, $g_{Zff}^L = e(2s_W^2 - 1)/(2c_W s_W)$ and $g_{Wff\nu_f}^R = 0$, $g_{Zff}^R = es_W/c_W$.

Other form factors can be obtained as follows.

$$F_{1L} = F_{2L}(\{q_{13}, q_{23}\} \rightarrow \{q_{23}, q_{13}\}), \tag{38}$$

$$F_{kR} = F_{kL}(g_{Wff\nu_f}^L \rightarrow g_{Wff\nu_f}^R; g_{Zff}^L \rightarrow g_{Zff}^R) \tag{39}$$

for $k = 1, 2$.

It is stressed that we derive alternative results for the form factors of $H \rightarrow f\bar{f}\gamma$ in the SM in comparison with previous works, because our calculations are computed in the unitary gauge. Thus, our formulas may get different forms in comparison with the results in [20] which have been calculated in R_ξ -gauge. In this paper, we cross-check our results with [20] by numerical tests. The numerical results for this check

are shown in Table 2. We find that our results are in good agreement with the ones in [20] with more than 10 digits.

We also generate the decay widths for $H \rightarrow e\bar{e}\gamma$ and cross-check our results with [13]. The results are presented in Table 3. For this test, we adjust the input parameters and apply all cuts in the same way as in [13]. In the Table 3, the parameter k is taken into account which comes from the kinematical cuts of the invariant masses m_{ff} , $m_{f\gamma}$ as follows:

$$m_{ff}^2, m_{f\gamma}^2 \geq (kM_H)^2. \quad (40)$$

We find that our results are in good agreement with the ones in [13].

4.2 $U(1)_{B-L}$ extension of the SM

We refer to the appendix B for reviewing briefly this model. In the appendix B, all couplings relating to the decay processes $H \rightarrow f\bar{f}\gamma$ are derived in $U(1)_{B-L}$ extension of the SM (see Table 4). Apart from all particles in the SM, two additional neutral Higgs and a neutral gauge boson Z' which belongs to $U(1)_{B-L}$ gauge symmetry are taken into account in this model.

For phenomenological study, we have to include three the new parameters such as the mixing angle c_α , the $U(1)_{B-L}$ coupling g'_1 and the mass of new gauge boson $M'_{Z'}$. In all the below results, we set $c_\alpha = 0.3, 0.7$ and $c_\alpha = 1$ (for $c_\alpha = 1$,

we are back to the standard model case). The mass of Z' is in the range of $600 \text{ GeV} \leq M'_{Z'} \leq 1000 \text{ GeV}$. The coupling g'_1 is in $0.05 \leq g'_1 \leq 0.5$.

We study the impact of the $U(1)_{B-L}$ extension of the SM on the differential decay widths as functions of m_{ff} and $m_{f\gamma}$. The results are shown in the Fig. 13 with fixed $M'_{Z'} = 1000 \text{ GeV}$. In these figures, the solid line shows the SM case by setting $c_\alpha = 1$. While the dashed line presents $c_\alpha = 0.7$ and the dash-dotted line is for $c_\alpha = 0.3$. In the left figure, we observe the photon pole at the lowest region of m_{ff} . The decay rates decrease up to $m_{ff} \sim 60 \text{ GeV}$. They then grown up to the Z -peak (the peak of $Z \rightarrow f\bar{f}$) which is located around $m_{ff} \sim 90 \text{ GeV}$. Beyond the peak, the decay rates decrease rapidly. In the right figure, the decay widths increase up to the peak of $m_{f\gamma} \sim 81 \text{ GeV}$ which corresponds to the photon recoil mass at the Z -pole. They also decrease rapidly beyond the peak. It is interesting to find that the contributions of $U(1)_{B-L}$ extension are sizable in both cases of $c_\alpha = 0.7, 0.3$. These effects can be probed clearly at the future colliders.

We next examine the decay widths as a function of $M'_{Z'}$. In this study, we change the mass of Z' boson as $800 \text{ GeV} \leq M_{Z'} \leq 1000 \text{ GeV}$ and set $c_\alpha = 0.7$ (see Fig. 14). The dashed line shows the case of $g'_1 = 0.05$, the dotted line presents $g'_1 = 0.2$ and the dash-dotted line is for $g'_1 = 0.5$. In the whole range of $M'_{Z'}$, we observe that the decay widths

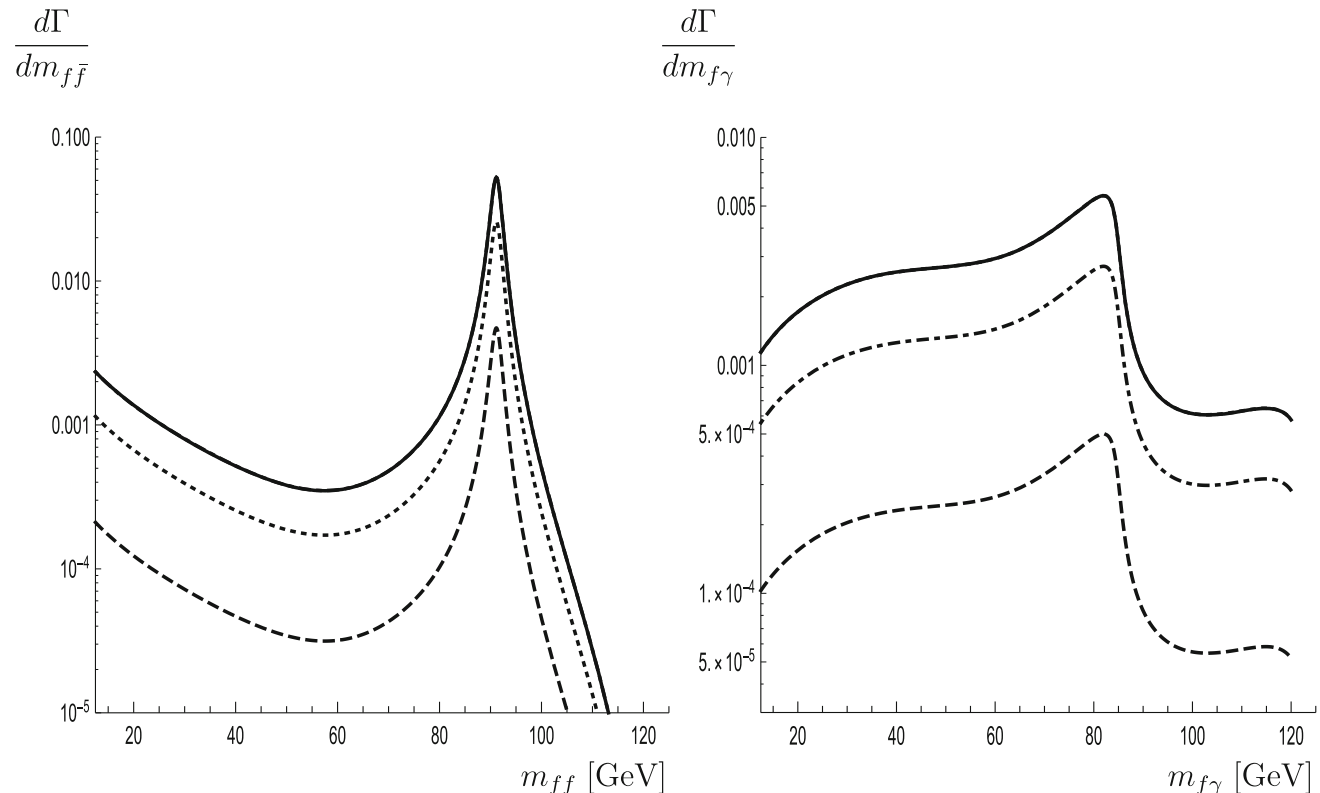


Fig. 13 Differential of the decay width as functions of m_{ff} and $m_{f\gamma}$

Fig. 14 The decay widths which are functions of $M'_{Z'}$

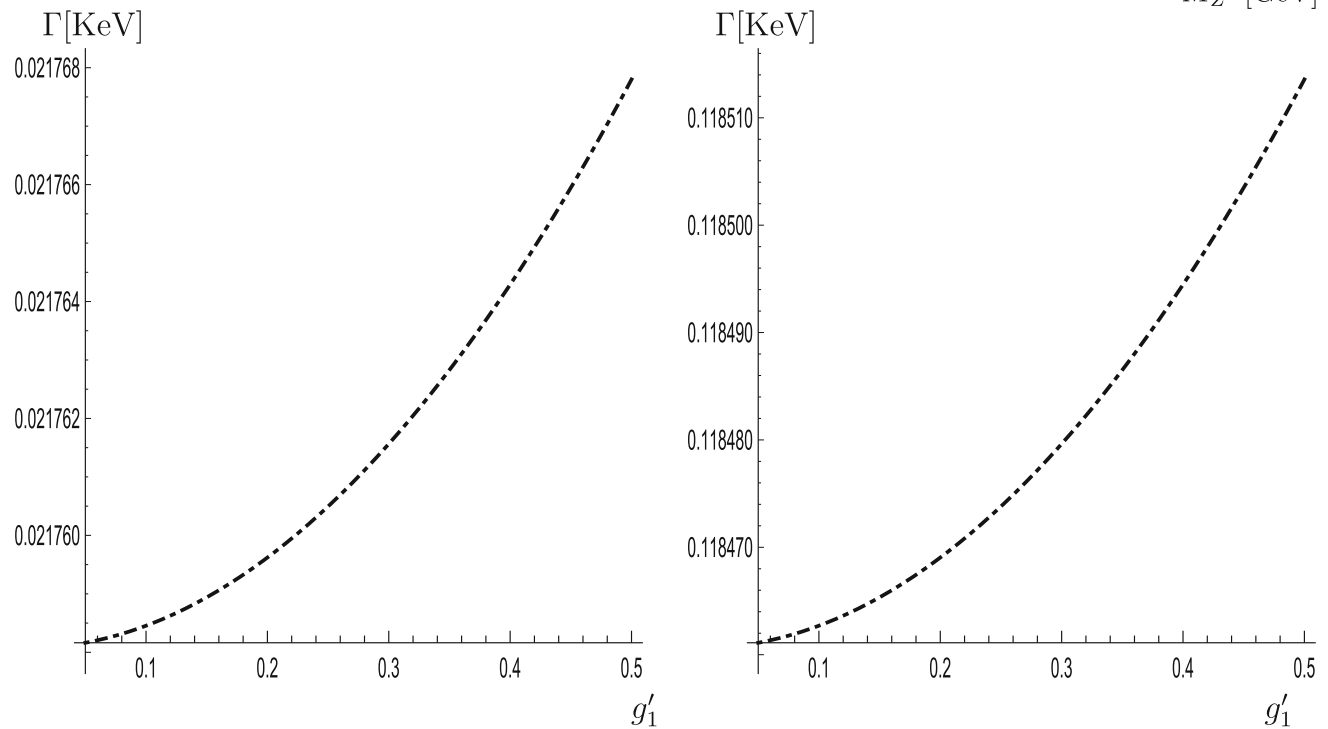
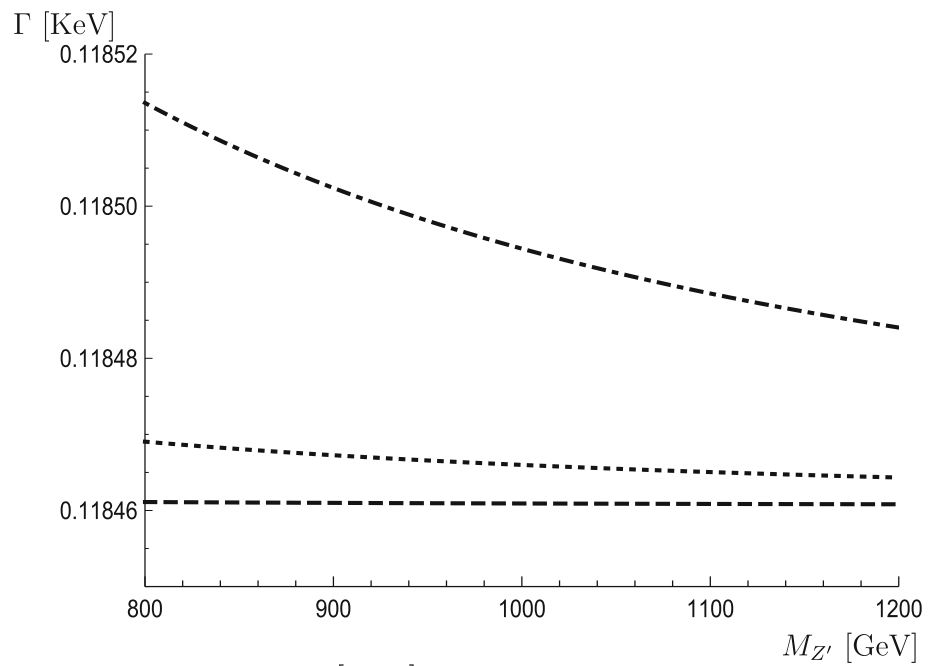


Fig. 15 The decay widths are function of g'_1

are proportional to g'_1 (it is also confirmed by later analyses). They also decrease with increasing $M'_{Z'}$. We observe that the contributions from the $U(1)_{B-L}$ extension are massive and can be probed clearly at future colliders.

We finally discuss the effect of g'_1 on the decay widths (seen Fig. 15). In these figures, we set $M'_{Z'} = 800$ GeV and $c_\alpha = 0.3$ ($c_\alpha = 0.7$) for the left figure (for the right figure)

respectively. We find that the decay widths are proportional to g'_1 .

4.3 Two Higgs doublet model

For reviewing the THDM, we refer to the appendix C for more detail. In this framework, the gauge sector is the same as in the SM. It means that we have $V_i = V_j = W$, $V_k^0 = Z, \gamma$.

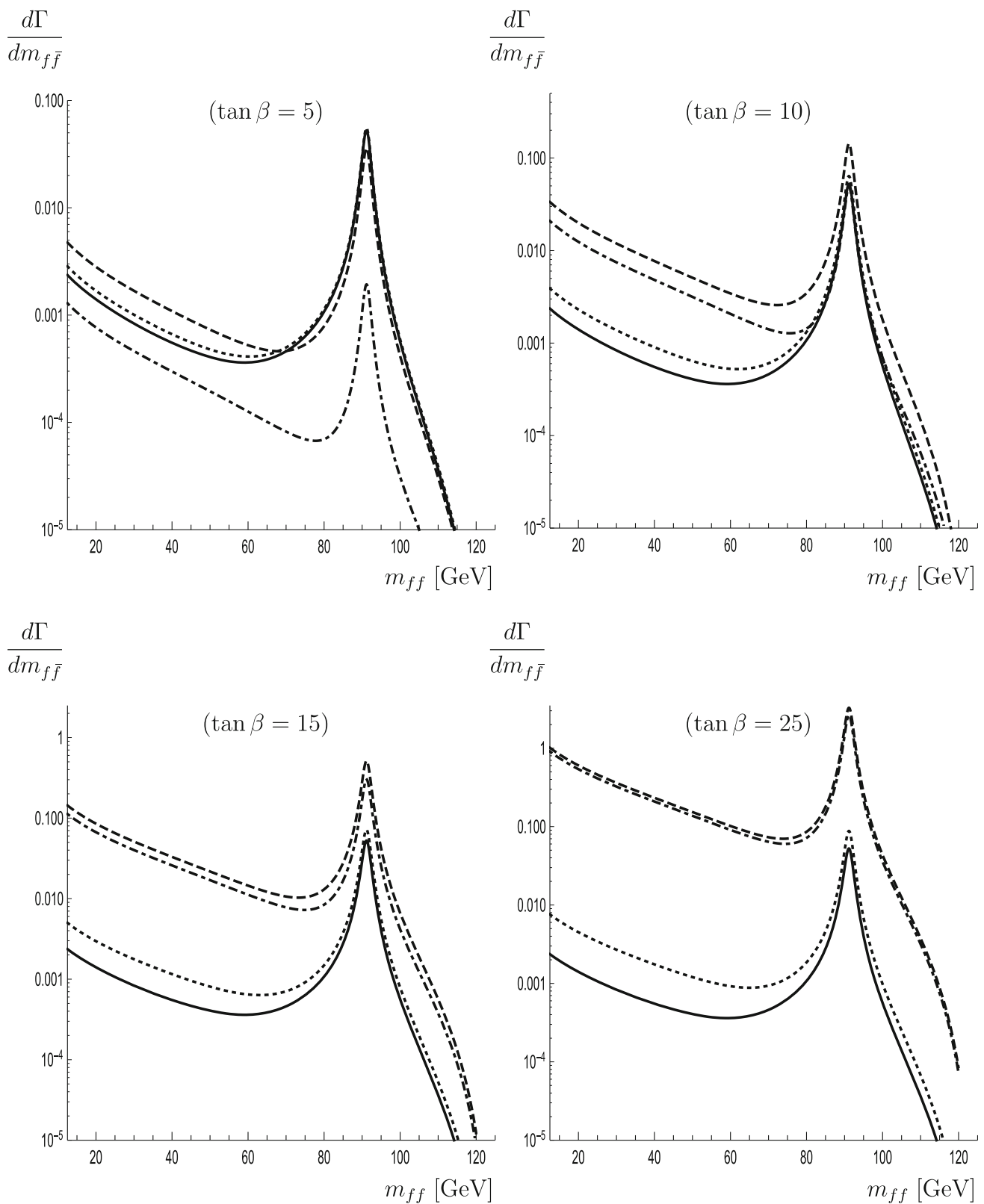


Fig. 16 Differential decay rates as a function of the invariant mass of leptons m_{ff} with changing $\alpha = -0.4\pi, 0, 0.4\pi$

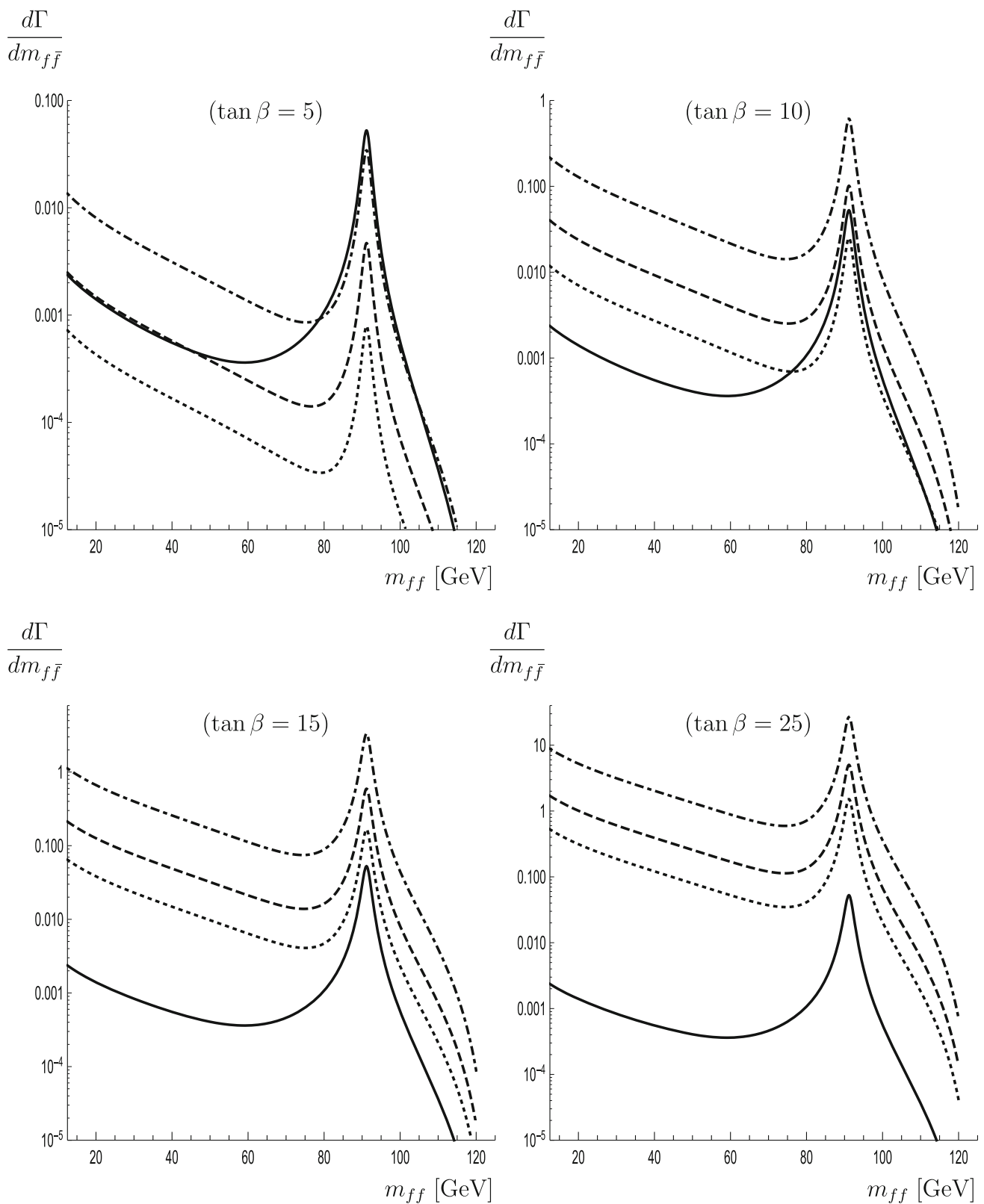


Fig. 17 Differential decay rates as a function of the invariant mass of leptons m_{ff} with changing charged Higgs masses $M_{H^\pm} = 400, 600, 800$ GeV

In the Higgs sectors, one has additional charged Higgs H^\pm and two neutral scalar CP even Higgs bosons H_1^0, H_2^0 and a CP odd Higgs A . All couplings relating to the decay processes $H \rightarrow f \bar{f} \gamma$ are shown in Table 5.

For the phenomenological results, we take $1 \leq \tan \beta \leq 30$, $M_{H^0} = 125.1 \text{ GeV}$, $-900^2 \text{ GeV}^2 \leq m_{12}^2 \leq 900^2 \text{ GeV}^2$, $340 \text{ GeV} \leq M_{H^\pm} \leq 900 \text{ GeV}$, $-\pi/2 \leq \alpha \leq \pi/2$. We study the differential decay rates as a function of the invariant mass of leptons m_{ff} . We select $M_{H^\pm} = 700 \text{ GeV}$, $m_{12}^2 = 800^2 \text{ GeV}^2$. The results are shown in Fig. 16. In this figure, the solid line shows the SM case. The dashed line presents the case of $\alpha = -0.4\pi$. The dash-dotted line is for the case of $\alpha = 0$. The dotted line is for the case of $\alpha = 0.4\pi$. The values of $\tan \beta$ ($\tan \beta = 5, 10, 15$ and 25) are shown directly in the sub-figures of Fig. 16. The decay rates have the same behavior as in previous cases. We observe the photon pole at the lowest region of m_{ff} . They decrease from the photon pole to the region of $m_{ff} \sim 60 \text{ GeV}$ and then grown up to the Z -peak. Beyond the Z -peak, the decay rates decrease rapidly. The effect of the THDM are also visible in all cases.

We next change the charged Higgs masses $M_{H^\pm} = 400, 600, 800 \text{ GeV}$ and take $\alpha = 0.4\pi$. In this figure, the solid line shows the SM case. The dash-dotted line is for the case of $M_{H^\pm} = 400 \text{ GeV}$. The dashed line presents the case of $M_{H^\pm} = 600 \text{ GeV}$. The dotted line is for the case of $M_{H^\pm} = 800 \text{ GeV}$. The values of $\tan \beta$ ($\tan \beta = 5, 10, 15$ and 25) are shown directly in the sub-figures of Fig. 17. The decay widths are inversely proportional to the charged Higgs masses. We find that the effect of the THDM are sizeable contributions in all the above cases. These effects can be discriminated clearly at future colliders.

5 Conclusions

We have performed the calculations for one-loop contributions to the decay processes $H \rightarrow f \bar{f} \gamma$ in the limit of $m_f \rightarrow 0$. In this computation, we have considered all possible contributions of the additional heavy vector gauge bosons, heavy fermions, and charged (and also neutral) scalar particles that may exchange in the loop diagrams. The analytic formulas are written in terms of Passarino-Veltman functions that can be evaluated numerically by using the package `LoopTools`. The evaluations have then been applied to the Standard Model, $U(1)_{B-L}$ extension of the SM, the Two-Higgs-Doublet Model. Phenomenological results of the decay processes for the above models have been studied in detail. We find that the effects of new physics are sizable contributions and they can be probed at future colliders.

Acknowledgements This research is funded by Vietnam National Foundation for Science and Technology Development (NAFOSTED)

under the grant number 103.01-2019.346. K.H. Phan would like to thank Dr. L.T. Hue for helpful discussions.

Data Availability Statement This manuscript has no associated data or the data will not be deposited. [Authors' comment: This is theoretical work, we present analytic results in this work. Therefore, we have not used any data.]

Open Access This article is licensed under a Creative Commons Attribution 4.0 International License, which permits use, sharing, adaptation, distribution and reproduction in any medium or format, as long as you give appropriate credit to the original author(s) and the source, provide a link to the Creative Commons licence, and indicate if changes were made. The images or other third party material in this article are included in the article's Creative Commons licence, unless indicated otherwise in a credit line to the material. If material is not included in the article's Creative Commons licence and your intended use is not permitted by statutory regulation or exceeds the permitted use, you will need to obtain permission directly from the copyright holder. To view a copy of this licence, visit <http://creativecommons.org/licenses/by/4.0/>.

Funded by SCOAP³.

Appendix A: Tensor one-loop reductions

In this appendix, tensor one-loop reduction method in [48] is discussed briefly. First, the definition of one-loop one-, two-, three- and four-point tensor integrals with rank R are as follows:

$$\{A; B; C; D\}^{\mu_1 \mu_2 \dots \mu_R} = (\mu^2)^{2-d/2} \int \frac{d^d k}{(2\pi)^d} \frac{k^{\mu_1} k^{\mu_2} \dots k^{\mu_R}}{\{P_1; P_1 P_2; P_1 P_2 P_3; P_1 P_2 P_3 P_4\}}. \tag{A.1}$$

In this formula, P_j ($j = 1, \dots, 4$) are the inverse Feynman propagators

$$P_j = (k + q_j)^2 - m_j^2 + i\rho. \tag{A.2}$$

In this equation, we use $q_j = \sum_{i=1}^j p_i$ with p_i for the external momenta, and m_j for internal masses in the loops. Dimensional regularization is performed in space-time dimension $d = 4 - 2\epsilon$. The parameter μ^2 plays the role of a renormalization scale. When the numerator of the integrands in Eq. (A.1) becomes 1, one has the corresponding scalar one-loop functions (they are noted as A_0, B_0, C_0 and D_0). Explicit reduction formulas for one-loop one-, two-, three- and four-point tensor integrals up to rank $R = 3$ are written as follows [48]. In particular, for one- and two-point tensor integrals, the reduction formulas are:

$$A^\mu = 0, \tag{A.3}$$

$$A^{\mu\nu} = g^{\mu\nu} A_{00}, \tag{A.4}$$

$$A^{\mu\nu\rho} = 0, \tag{A.5}$$

$$B^\mu = q^\mu B_1, \tag{A.6}$$

$$B^{\mu\nu} = g^{\mu\nu} B_{00} + q^\mu q^\nu B_{11}, \tag{A.7}$$

$$B^{\mu\nu\rho} = \{g, q\}^{\mu\nu\rho} B_{001} + q^\mu q^\nu q^\rho B_{111}, \tag{A.8}$$

For three-point functions, one has

$$C^\mu = q_1^\mu C_1 + q_2^\mu C_2 = \sum_{i=1}^2 q_i^\mu C_i, \tag{A.9}$$

$$C^{\mu\nu} = g^{\mu\nu} C_{00} + \sum_{i,j=1}^2 q_i^\mu q_j^\nu C_{ij}, \tag{A.10}$$

$$C^{\mu\nu\rho} = \sum_{i=1}^2 \{g, q_i\}^{\mu\nu\rho} C_{00i} + \sum_{i,j,k=1}^2 q_i^\mu q_j^\nu q_k^\rho C_{ijk}, \tag{A.11}$$

Similarly, tensor reduction formulas for four-point functions are given by

$$D^\mu = q_1^\mu D_1 + q_2^\mu D_2 + q_3^\mu D_3 = \sum_{i=1}^3 q_i^\mu D_i, \tag{A.12}$$

$$D^{\mu\nu} = g^{\mu\nu} D_{00} + \sum_{i,j=1}^3 q_i^\mu q_j^\nu D_{ij}, \tag{A.13}$$

$$D^{\mu\nu\rho} = \sum_{i=1}^3 \{g, q_i\}^{\mu\nu\rho} D_{00i} + \sum_{i,j,k=1}^3 q_i^\mu q_j^\nu q_k^\rho D_{ijk}. \tag{A.14}$$

The short notation [48] $\{g, q_i\}^{\mu\nu\rho}$ is used as follows: $\{g, q_i\}^{\mu\nu\rho} = g^{\mu\nu} q_i^\rho + g^{\nu\rho} q_i^\mu + g^{\mu\rho} q_i^\nu$ in the above relations. The scalar coefficients $A_{00}, B_1, \dots, D_{333}$ in the right hand sides of the above equations are so-called Passarino-Veltman functions [48]. They have been implemented into `LoopTools` [25] for numerical computations.

Appendix B: Review of $U(1)_{B-L}$ extension

In this appendix, we review briefly $U(1)_{B-L}$ extension [26]. This model follows gauge symmetry $SU(3)_C \otimes SU(2)_L \otimes U(1)_Y \otimes U(1)_{B-L}$. By including complex scalar S , general scalar potential is given by

$$V(\Phi, S) = m^2 \Phi^\dagger \Phi + \lambda_1 (\Phi^\dagger \Phi)^2 + \mu^2 |S|^2 + \lambda_2 |S|^4 + \lambda_3 \Phi^\dagger \Phi |S|^2. \tag{B.1}$$

In order to find mass spectrum of the scalar sector, we expand the scalar fields around their vacuum as follows:

$$\Phi = \begin{pmatrix} \phi^+ \\ v_\phi + h + i\xi \end{pmatrix}, \quad S = \frac{v_s + h' + i\xi'}{\sqrt{2}}. \tag{B.2}$$

The Goldstone bosons ϕ^\pm, ξ will give the masses of W^\pm and Z bosons. In unitary gauge, the mass eigenvalues of neutral Higgs are given:

$$\begin{pmatrix} h_1 \\ h_2 \end{pmatrix} = \begin{pmatrix} c_\alpha & -s_\alpha \\ s_\alpha & c_\alpha \end{pmatrix} \begin{pmatrix} h \\ h' \end{pmatrix} \tag{B.3}$$

with mixing angle

$$s_{2\alpha} = \sin 2\alpha = \frac{\lambda_3 v_\phi v_s}{\sqrt{(\lambda_1 v_\phi^2 - \lambda_2 v_s^2)^2 + (\lambda_3 v_\phi v_s)^2}} \tag{B.4}$$

After this transformation, masses of scalar Higgs are given

$$M_{h_1}^2 = \lambda_1 v_\phi^2 + \lambda_2 v_s^2 - \sqrt{(\lambda_1 v_\phi^2 - \lambda_2 v_s^2)^2 + (\lambda_3 v_\phi v_s)^2}, \tag{B.5}$$

$$M_{h_2}^2 = \lambda_1 v_\phi^2 + \lambda_2 v_s^2 + \sqrt{(\lambda_1 v_\phi^2 - \lambda_2 v_s^2)^2 + (\lambda_3 v_\phi v_s)^2}. \tag{B.6}$$

The masses of the gauge bosons W, Z and Z' are obtained by expanding the following kinematic terms

$$\mathcal{L}_{\text{gauge}} \rightarrow (D^\mu \Phi)^\dagger D_\mu \Phi, \quad (D^\mu S)^\dagger D_\mu S. \tag{B.7}$$

As a result, the mass of Z' is $M_{Z'} = 2v_s g_1'$.

The Yukawa interactions involving right-handed neutrinos are given:

$$\begin{aligned} \mathcal{L}_Y = & -y_{jk}^d \bar{q}_{Lj} d_{Rk} \Phi - y_{jk}^u \bar{q}_{Lj} u_{Rk} i\sigma_2 \Phi^* - y_{jk}^e \bar{l}_{Lj} e_{Rk} \Phi \\ & - y_{jk}^\nu \bar{l}_{Lj} \nu_{Rk} i\sigma_2 \Phi^* - y_{jk}^M \overline{(\nu_R)}_j^c \nu_{Rk} S + \text{h.c.} \end{aligned} \tag{B.8}$$

for $j, k = 1, 2, 3$. The last term in this equation is the Majorana mass term for right-handed neutrinos. After the spontaneous symmetry-breaking, the mass matrix of neutrinos is

$$M = \begin{pmatrix} 0 & m_D = \frac{(y^\nu)^*}{\sqrt{2}} v_\phi \\ m_D^T & M = \sqrt{2} y^M v_s \end{pmatrix}. \tag{B.9}$$

The diagonalization is obtained by the transformation

$$\text{diag}\left(-\frac{(m_D^i)^2}{M^i}, M^i\right) = \begin{pmatrix} \cos \alpha_i & -\sin \alpha_i \\ \sin \alpha_i & \cos \alpha_i \end{pmatrix} \begin{pmatrix} 0 & m_D^i \\ m_D^i & M^i \end{pmatrix} \begin{pmatrix} \cos \alpha_i & \sin \alpha_i \\ -\sin \alpha_i & \cos \alpha_i \end{pmatrix} \tag{B.10}$$

for $i = 1, 2, 3$ and $\alpha_i = \arcsin(m_D^i/M^i)$.

We show all relevant couplings in the decay under consideration. In the case of $\alpha_i \rightarrow 0$, all the couplings are shown in Table 4

Table 4 All the couplings involving the decay processes $H \rightarrow f \bar{f} \gamma$ in the $U(1)_{B-L}$ extension of the SM

Vertices	Couplings
$h_1(h_2) f \bar{f}$	$-i \frac{c_\alpha(s_\alpha) e m_f}{2M_{W_S W}}$
$Z'_\mu f \bar{f}$	$i Q_f g_1' \gamma_\mu$
$h_1(h_2) W_\mu^+ W_\nu^-$	$i \frac{e M_W}{s_W} c_\alpha(s_\alpha) g_{\mu\nu}$
$h_1(h_2) Z_\mu Z_\nu$	$i \frac{e M_W}{c_W s_W} c_\alpha(s_\alpha) g_{\mu\nu}$
$h_1(h_2) Z'_\mu Z'_\nu$	$-i 4g_1' M_Z' s_\alpha (-c_\alpha) g_{\mu\nu}$

Appendix C: Review of two Higgs doublet model

Based on Ref. [27], we review briefly the two Higgs doublet model with softly-broken Z_2 -symmetry. In this model, there are two scalar doublets Φ_1, Φ_2 with hypercharge $Y = 1/2$. Parts of the Lagrangian extended from the SM are presented as follows:

$$\mathcal{L} = \mathcal{L}_K + \mathcal{L}_Y - V(\Phi_1, \Phi_2), \tag{C.1}$$

where the kinematic term is \mathcal{L}_K , the Yukawa part is \mathcal{L}_Y and $V(\Phi_1, \Phi_2)$ is the Higgs potential. First, the kinematic term takes the form of

$$\mathcal{L}_K = \sum_{k=1}^2 (D_\mu \Phi_k)^\dagger (D^\mu \Phi_k) \tag{C.2}$$

with $D_\mu = \partial_\mu - igT^a W_\mu^a - i\frac{g'}{2}B_\mu$. The Higgs potential with broken the Z_2 -symmetry is expressed:

$$\begin{aligned} V(\Phi_1, \Phi_2) = & \frac{1}{2}m_{11}^2 \Phi_1^\dagger \Phi_1 - m_{12}^2 (\Phi_1^\dagger \Phi_2 \\ & + \Phi_2^\dagger \Phi_1) + \frac{1}{2}m_{22}^2 \Phi_2^\dagger \Phi_2 + \frac{\lambda_1}{2} (\Phi_1^\dagger \Phi_1)^2 \\ & + \frac{\lambda_2}{2} (\Phi_2^\dagger \Phi_2)^2 \\ & + \lambda_3 (\Phi_1^\dagger \Phi_1) (\Phi_2^\dagger \Phi_2) \\ & + \lambda_4 (\Phi_1^\dagger \Phi_2) (\Phi_2^\dagger \Phi_1) \\ & + \frac{\lambda_5}{2} \left[(\Phi_1^\dagger \Phi_2)^2 + (\Phi_2^\dagger \Phi_1)^2 \right]. \end{aligned} \tag{C.3}$$

In this potential, m_{12}^2 plays the role of soft-breaking scale of the Z_2 -symmetry. The two scalar doublet fields can be parameterized as follows:

$$\Phi_1 = \begin{pmatrix} \phi_1^+ \\ \frac{v_1 + \eta_1 + i\xi_1}{\sqrt{2}} \end{pmatrix}, \quad \Phi_2 = \begin{pmatrix} \phi_2^+ \\ \frac{v_2 + \eta_2 + i\xi_2}{\sqrt{2}} \end{pmatrix}. \tag{C.4}$$

We get an equation system for these parameters from the stationary conditions of the Higgs potential. The relations are shown as follows:

$$m_{11}^2 - \mu^2 \frac{v_2^2}{v^2} + \frac{\lambda_1}{2} v_1^2 + \frac{\lambda_{345}}{2} v_2^2 = 0, \tag{C.5}$$

$$m_{22}^2 - \mu^2 \frac{v_1^2}{v^2} + \frac{\lambda_2}{2} v_2^2 + \frac{\lambda_{345}}{2} v_1^2 = 0, \tag{C.6}$$

where $v^2 = v_1^2 + v_2^2$ is fixed at the electroweak scale or $v = (\sqrt{2}G_F)^{-1/2} = 246$ GeV and the new parameter μ^2 is defined as $\mu^2 = \frac{v^2}{v_1 v_2} m_{12}^2$. The shorten notation is $\lambda_{345} = \lambda_3 + \lambda_4 + \lambda_5$. The mixing angle is given $t_\beta = \tan \beta = v_2/v_1$. The mass terms of the Higgs potential V_{mass} can be expressed

as:

$$\begin{aligned} V_{mass} = & (\phi_1^+, \phi_2^+) R_\beta \begin{pmatrix} 0 & 0 \\ 0 & M_{H^+}^2 \end{pmatrix} R_\beta^{-1} \begin{pmatrix} \phi_1^+ \\ \phi_2^+ \end{pmatrix} \\ & + \frac{1}{2} (\xi_1, \xi_2) R_\beta \begin{pmatrix} 0 & 0 \\ 0 & M_A^2 \end{pmatrix} R_\beta^{-1} \begin{pmatrix} \xi_1 \\ \xi_2 \end{pmatrix} \\ & + \frac{1}{2} (\eta_1, \eta_2) R_\beta \begin{pmatrix} M_{H^0}^2 & 0 \\ 0 & M_{H_1^0}^2 \end{pmatrix} R_\beta^{-1} \begin{pmatrix} \eta_1 \\ \eta_2 \end{pmatrix}. \end{aligned} \tag{C.7}$$

Here the diagonalized matrix of neutral masses is defined as $\text{diag}(M_{H_2^0}^2, M_{H_1^0}^2) = R_\alpha \mathcal{M}^2 R_\alpha^T$, with $(\mathcal{M}^2)_{ij} = \frac{\partial^2 V}{\partial \eta_i \partial \eta_j}$. (C.8)

The mass eigenstates can be then expressed as follows:

$$\begin{aligned} \begin{pmatrix} G^+ \\ H^+ \end{pmatrix} &= R_\beta^{-1} \begin{pmatrix} \phi_1^+ \\ \phi_2^+ \end{pmatrix}, \\ \begin{pmatrix} G^0 \\ A \end{pmatrix} &= R_\beta^{-1} \begin{pmatrix} \xi_1 \\ \xi_2 \end{pmatrix}, \quad \begin{pmatrix} H_2^0 \\ H_1^0 \end{pmatrix} = R_\alpha^{-1} R_\beta^{-1} \begin{pmatrix} \eta_1 \\ \eta_2 \end{pmatrix} \end{aligned} \tag{C.9}$$

where

$$R_\beta = \begin{pmatrix} c_\beta & s_\beta \\ -s_\beta & c_\beta \end{pmatrix}, \quad R_\alpha = \begin{pmatrix} c_\alpha & s_\alpha \\ -s_\alpha & c_\alpha \end{pmatrix} \tag{C.10}$$

with $-\pi/2 \leq \alpha \leq \pi/2$. In the unitary gauge, it is well-known that G^+ and G^0 are massless Goldstone bosons that will become the longitudinal polarization of W^+ and Z^0 . The remains H^\pm, A and $H_{1,2}^0$ become the charged Higgs bosons, a CP-odd Higgs boson and CP-even Higgs bosons respectively. The masses of these scalar bosons are given by

$$M_{H^\pm}^2 = \mu^2 - \frac{v^2}{2} (\lambda_4 + \lambda_5), \tag{C.11}$$

$$M_A^2 = \mu^2 - v^2 \lambda_5, \tag{C.12}$$

$$M_{H_1^0}^2 = s_\alpha^2 \mathcal{M}_{11}^2 - 2s_\alpha c_\alpha \mathcal{M}_{12}^2 + c_\alpha^2 \mathcal{M}_{22}^2, \tag{C.13}$$

$$M_{H_2^0}^2 = c_\alpha^2 \mathcal{M}_{11}^2 + 2s_\alpha c_\alpha \mathcal{M}_{12}^2 + s_\alpha^2 \mathcal{M}_{22}^2. \tag{C.14}$$

From the Higgs potential in Eq. (C.3) with the stationary conditions in (C.5), we have 7 parameters. They are

$$\{\lambda_{1,2,3,4,5}, t_\beta, m_{12}^2\}. \tag{C.15}$$

For phenomenological analyses, the above parameters are transferred to the following parameters:

$$\{M_{H^+}^2, M_A^2, M_{H_1^0}^2, M_{H_2^0}^2, \alpha, t_\beta, m_{12}^2\}. \tag{C.16}$$

All the couplings that are involved in the decay processes $H \rightarrow f \bar{f} \gamma$ are derived in this appendix. In general, we can consider the lightest Higgs boson H_1^0 is the SM like-Higgs boson. In Table 5, all the couplings are shown in detail.

For the Yukawa part, we refer [27] for more detail. Depend on the types of the THDMs, we then have the couplings of scalar fields and fermions.

Table 5 All the couplings that are involved in the decay processes $H \rightarrow f \bar{f} \gamma$ in the THDM

Vertices	Couplings
$H_1^0 W_\mu^+ W_\nu^-$	$i \frac{2M_W^2}{v} s(\beta-\alpha) g_{\mu\nu}$
$H_1^0 Z_\mu Z_\nu$	$i \frac{2M_Z^2}{v} s(\beta-\alpha) g_{\mu\nu}$
$H_1^0(p) H^\pm(q) W_\mu^\mp$	$\mp i \frac{M_W}{v} c(\beta-\alpha) (p-q)_\mu$
$H^+(p) H^-(q) A_\mu$	$i \frac{2M_W}{v} s_W (p-q)_\mu$
$H^+(p) H^-(q) Z_\mu$	$i \frac{M_Z}{v} c_{2W} (p-q)_\mu$
$H_1^0 H^+ H^-$	$\frac{i}{v} [(2\mu^2 - 2M_{H^\pm}^2 - M_{H_1^0}^2) s(\beta-\alpha) + 2(\mu^2 - M_{H_1^0}^2) \cot 2\beta c(\beta-\alpha)]$
$H^+ H^- A_\mu A_\nu$	$2ie^2 g_{\mu\nu}$
$H^+ H^- Z_\mu A_\nu$	$ieg \frac{c_{2W}}{c_W} g_{\mu\nu}$

Table 6 Feynman rules involving the decay channels in the unitary gauge

Particle types	Propagators
Fermions f	$i \frac{k + m_f}{k^2 - m_f^2}$
Charged (neutral) gauge bosons $V_i(V_i^0)$	$\frac{-i}{p^2 - M_{V_i}^2(M_{V_i^0}^2)} \left[g^{\mu\nu} - \frac{p^\mu p^\nu}{M_{V_i}^2(M_{V_i^0}^2)} \right]$
Gauge boson V_k^{0*} poles	$\frac{-i}{p^2 - M_{V_k}^2 + i\Gamma_{V_k} M_{V_k^0}} \left[g^{\mu\nu} - \xi_{V_k^0} \frac{p^\mu p^\nu}{M_{V_k}^2} \right]$
Charged (neutral) scalar bosons $S_i(S_i^0)$	$\frac{i}{p^2 - M_{S_i}^2(M_{S_i^0}^2)}$

$$\mathcal{L}_{H_1^0 \bar{t} t} = -\frac{m_t}{v} \frac{c_\alpha}{s_\beta} \bar{t} t H_1^0. \tag{C.17}$$

Appendix D: Feynman rules and couplings

In the below Tables 6 and 7, we use $P_{L/R} = (1 \mp \gamma_5)/2$, $\Gamma^{\mu\nu\lambda}(p_1, p_2, p_3) = g^{\mu\nu}(p_1 - p_2)^\lambda + g^{\lambda\nu}(p_2 - p_3)^\mu + g^{\mu\lambda}(p_3 - p_1)^\nu$ and $S^{\mu\nu,\alpha\beta} = 2g^{\mu\nu}g^{\alpha\beta} - g^{\mu\alpha}g^{\nu\beta} - g^{\mu\beta}g^{\nu\alpha}$ and Q_V denotes the electric charge of the gauge bosons V_i, V_j and Q_S is charge of the charged Higgs bosons S_i, S_j . Moreover, the factor $\xi_{V_k^0}$ is included for covering all possible cases of neutral gauge boson. It can be 0 and 1 for the case of the pole of photon and Z-boson (Z' -boson) respectively.

Table 7 All couplings that are involved in the decay processes in unitary gauge

Vertices	Couplings
$H \cdot S_i \cdot S_j$	$-i g_{HS_i S_j}$
$H \cdot S_i^0 \cdot S_j^0$	$-i g_{HS_i^0 S_j^0}$
$H \cdot V_i^\mu \cdot V_j^\nu$	$i g_{HV_i V_j} g^{\mu\nu}$
$H \cdot V_i^{0\mu} \cdot V_j^{0\nu}$	$i g_{HV_i^0 V_j^0} g^{\mu\nu}$
$H \cdot \bar{f}_i \cdot f_j$	$-i (g_{Hf_i f_j}^L P_L + g_{Hf_i f_j}^R P_R)$
$S_k^0 \cdot \bar{f} \cdot f$	$-i (g_{S_k^0 f f}^L P_L + g_{S_k^0 f f}^R P_R)$
$A^\mu \cdot f_i \cdot \bar{f}_i$	$ie Q_f \gamma^\mu$
$H(p) \cdot V_i^\mu \cdot S_j(q)$	$i g_{HV_i S_j} (p-q)^\mu$
$H(p) \cdot V_i^{0\mu} \cdot S_j^0(q)$	$i g_{HV_i^0 S_j^0} (p-q)^\mu$
$V_k^{0\mu} \cdot V_i^\nu \cdot S_j^\pm$	$\pm i g_{V_k^0 V_i S_j} g^{\mu\nu}$
$V_k^{0\mu}(p_1) \cdot V_i^\nu(p_2) \cdot V_j^\lambda(p_3)$	$-i g_{V_k^0 V_i V_j} \Gamma_{\mu\nu\lambda}(p_1, p_2, p_3)$
$A^\mu(p_1) \cdot V_i^\nu(p_2) \cdot V_j^\lambda(p_3)$	$-ie Q_V \Gamma^{\mu\nu\lambda}(p_1, p_2, p_3)$
$V_k^{0\mu} \cdot f_i \cdot \bar{f}_j$	$i \gamma^\mu (g_{V_k^0 f_i f_j}^L P_L + g_{V_k^0 f_i f_j}^R P_R)$
$V_k^{0\mu} \cdot A^\nu \cdot V_i^\alpha \cdot V_j^\beta$	$-ie Q_V g_{V_k^0 A V_i V_j} S_{\mu\nu,\alpha\beta}$
$V_k^{0\mu} \cdot A^\nu \cdot S_i \cdot S_j$	$-ie Q_S g_{V_k^0 A S_i S_j} g_{\mu\nu}$
$V_k^{0\mu} \cdot S_i(p) \cdot S_j(q)$	$i g_{V_k^0 S_i S_j} (p-q)^\mu$
$A^\mu \cdot S_i \cdot S_i$	$ie Q_S (p-q)^\mu$
$V_i^\mu \cdot f \cdot \nu_f$	$i \gamma^\mu (g_{V_i f \nu_f}^L P_L + g_{V_i f \nu_f}^R P_R)$
$V_i^{0\mu} \cdot f \cdot f$	$i \gamma^\mu (g_{V_i^0 f f}^L P_L + g_{V_i^0 f f}^R P_R)$
$S_i \cdot \bar{f} \cdot \nu_f$	$i g_{S_i f \nu_f}^L P_L + i g_{S_i f \nu_f}^R P_R$
$S_i^* \cdot f \cdot \bar{\nu}_f$	$i g_{S_i^* f \nu_f}^R P_L + i g_{S_i^* f \nu_f}^L P_R$

References

1. G. Aad et al., ATLAS, Phys. Lett. B **716**, 1–29 (2012). <https://doi.org/10.1016/j.physletb.2012.08.020>
2. S. Chatrchyan et al., CMS, Phys. Lett. B **716**, 30–61 (2012). <https://doi.org/10.1016/j.physletb.2012.08.021>
3. A. Liss et al. [ATLAS], [arXiv:1307.7292](https://arxiv.org/abs/1307.7292) [hep-ex]
4. CMS, [arXiv:1307.7135](https://arxiv.org/abs/1307.7135) [hep-ex]
5. H. Baer, T. Barklow, K. Fujii, Y. Gao, A. Hoang, S. Kanemura, J. List, H.E. Logan, A. Nomerotski, M. Perelstein, et al. [arXiv:1306.6352](https://arxiv.org/abs/1306.6352) [hep-ph]
6. V. Khachatryan et al., CMS, Phys. Lett. B **753**, 341–362 (2016). <https://doi.org/10.1016/j.physletb.2015.12.039>
7. A.M. Sirunyan et al., CMS, JHEP **09**, 148 (2018). [https://doi.org/10.1007/JHEP09\(2018\)148](https://doi.org/10.1007/JHEP09(2018)148). [arXiv:1712.03143](https://arxiv.org/abs/1712.03143) [hep-ex]
8. A.M. Sirunyan et al., CMS, JHEP **11**, 152 (2018). [https://doi.org/10.1007/JHEP11\(2018\)152](https://doi.org/10.1007/JHEP11(2018)152). [arXiv:1806.05996](https://arxiv.org/abs/1806.05996) [hep-ex]
9. G. Aad et al., ATLAS, Phys. Lett. B **819**, 136412 (2021). <https://doi.org/10.1016/j.physletb.2021.136412>. [arXiv:2103.10322](https://arxiv.org/abs/2103.10322) [hep-ex]
10. Chen, L.B., Qiao, C.F., Zhu, R.L. Phys. Lett. B **726** (2013), 306–311 (Erratum: Phys. Lett. B **808** (2020), 135629). <https://doi.org/10.1016/j.physletb.2013.08.050>. [arXiv:1211.6058](https://arxiv.org/abs/1211.6058) [hep-ph]
11. J.S. Gainer, W.Y. Keung, I. Low, P. Schwaller, Phys. Rev. D **86**, 033010 (2012). <https://doi.org/10.1103/PhysRevD.86.033010>. [arXiv:1112.1405](https://arxiv.org/abs/1112.1405) [hep-ph]
12. A.Y. Korchin, V.A. Kovalchuk, Eur. Phys. J. C **74**(11), 3141 (2014). <https://doi.org/10.1140/epjc/s10052-014-3141-7>
13. A. Abbasabadi, D. Bowser-Chao, D.A. Dicus, W.W. Repko, Phys. Rev. D **52**, 3919–3928 (1995)
14. A. Djouadi, V. Driesen, W. Hollik, J. Rosiek, Nucl. Phys. B **491**, 68–102 (1997). [https://doi.org/10.1016/S0550-3213\(96\)00711-0](https://doi.org/10.1016/S0550-3213(96)00711-0)
15. A. Abbasabadi, W.W. Repko, Phys. Rev. D **62**, 054025 (2000). <https://doi.org/10.1103/PhysRevD.62.054025>. [arXiv:hep-ph/0004167](https://arxiv.org/abs/hep-ph/0004167)
16. D.A. Dicus, W.W. Repko, Phys. Rev. D **87**(7), 077301 (2013). <https://doi.org/10.1103/PhysRevD.87.077301>
17. Y. Sun, H.R. Chang, D.N. Gao, JHEP **05**, 061 (2013). [https://doi.org/10.1007/JHEP05\(2013\)061](https://doi.org/10.1007/JHEP05(2013)061)
18. G. Passarino, Phys. Lett. B **727**, 424–431 (2013). <https://doi.org/10.1016/j.physletb.2013.10.052>
19. D.A. Dicus, C. Kao, W.W. Repko, Phys. Rev. D **89**(3), 033013 (2014). <https://doi.org/10.1103/PhysRevD.89.033013>
20. A. Kachanovich, U. Nierste, I. Nišandžić, Phys. Rev. D **101**(7), 073003 (2020). <https://doi.org/10.1103/PhysRevD.101.073003>
21. N. Watanabe, Y. Kurihara, K. Sasaki, T. Uematsu, Phys. Lett. B **728**, 202–205 (2014). <https://doi.org/10.1016/j.physletb.2013.11.051>
22. N. Watanabe, Y. Kurihara, T. Uematsu, K. Sasaki, Phys. Rev. D **90**(3), 033015 (2014). <https://doi.org/10.1103/PhysRevD.90.033015>
23. C.S. Li, C.F. Qiao, S.H. Zhu, Phys. Rev. D **57**, 6928–6933 (1998). <https://doi.org/10.1103/PhysRevD.57.6928>
24. K. Sasaki, T. Uematsu, Phys. Lett. B **781**, 290–294 (2018). <https://doi.org/10.1016/j.physletb.2018.04.005>
25. T. Hahn, M. Perez-Victoria, Comput. Phys. Commun. **118**, 153–165 (1999)
26. L. Basso, A. Belyaev, S. Moretti, C.H. Shepherd-Themistocleous, Phys. Rev. D **80**, 055030 (2009). <https://doi.org/10.1103/PhysRevD.80.055030>
27. G.C. Branco, P.M. Ferreira, L. Lavoura, M.N. Rebelo, M. Sher, J.P. Silva, Phys. Rep. **516**, 1–102 (2012). <https://doi.org/10.1016/j.physrep.2012.02.002>
28. J.C. Pati, A. Salam, Phys. Rev. D **10**, 275–289 (1974) (Erratum: Phys. Rev. D **11**, 703–703 (1975))
29. R.N. Mohapatra, J.C. Pati, Phys. Rev. D **11**, 2558 (1975)
30. G. Senjanovic, R.N. Mohapatra, Phys. Rev. D **12**, 1502 (1975)
31. M. Singer, J.W.F. Valle, J. Schechter, Phys. Rev. D **22**, 738 (1980)
32. J.W.F. Valle, M. Singer, Phys. Rev. D **28**, 540 (1983)
33. F. Pisano, V. Pleitez, Phys. Rev. D **46**, 410–417 (1992)
34. P.H. Frampton, Phys. Rev. Lett. **69**, 2889–2891 (1992)
35. R.A. Diaz, R. Martinez, F. Ochoa, Phys. Rev. D **72**, 035018 (2005)
36. R.M. Fonseca, M. Hirsch, JHEP **08**, 003 (2016)
37. R. Foot, H.N. Long, T.A. Tran, Phys. Rev. D **50**(1), R34–R38 (1994)
38. L.A. Sanchez, F.A. Perez, W.A. Ponce, Eur. Phys. J. C **35**, 259–265 (2004)
39. W.A. Ponce, L.A. Sanchez, Mod. Phys. Lett. A **22**, 435–448 (2007)
40. Riazuddin and Fayyazuddin, Eur. Phys. J. C **56**, 389–394 (2008). [arXiv:0803.4267](https://arxiv.org/abs/0803.4267) [hep-ph]
41. A. Jaramillo, L.A. Sanchez, Phys. Rev. D **84**, 115001 (2011). [arXiv:1110.3363](https://arxiv.org/abs/1110.3363) [hep-ph]
42. H.N. Long, L.T. Hue, D.V. Loi, Phys. Rev. D **94**(1), 015007 (2016)
43. L. Michaels, F. Yu, JHEP **03**, 120 (2021). [https://doi.org/10.1007/JHEP03\(2021\)120](https://doi.org/10.1007/JHEP03(2021)120)
44. A. Barroso, J. Pulido, J.C. Romao, Nucl. Phys. B **267**, 509–530 (1986). [https://doi.org/10.1016/0550-3213\(86\)90128-8](https://doi.org/10.1016/0550-3213(86)90128-8)
45. D. Fontes, J.C. Romão, J.P. Silva, JHEP **12**, 043 (2014). [https://doi.org/10.1007/JHEP12\(2014\)043](https://doi.org/10.1007/JHEP12(2014)043)
46. L.T. Hue, A.B. Arbuzov, T.T. Hong, T.P. Nguyen, D.T. Si, H.N. Long, Eur. Phys. J. C **78**(11), 885 (2018). <https://doi.org/10.1140/epjc/s10052-018-6349-0>
47. H.H. Patel, Comput. Phys. Commun. **197**, 276–290 (2015)
48. A. Denner, S. Dittmaier, Nucl. Phys. B **734**, 62–115 (2006)
49. K.H. Phan, D.T. Tran, L. Hue, [arXiv:2106.14466](https://arxiv.org/abs/2106.14466) [hep-ph]